Investigating Basic Plasma Physics Issues in Laser-Produced Plasmas from the Relativistic to the Ultracold Regime

Andrea Macchi

CNR/INFM/polyLAB, Pisa
Dipartimento di Fisica "Enrico Fermi", Università di Pisa

www.df.unipi.it/~macchi/

LENS, Florence, February 3, 2009

Contributors

Francesco Ceccherini, Fulvio Cornolti,
Tatiana V. Liseykina*, Francesco Pegoraro

Dipartimento di Fisica “Enrico Fermi”,
Università di Pisa and CNISM, Pisa

**presently at Max Planck Institute*
for Nuclear Physics, Heidelberg, Germany

Alessandra Bigongiari, Carlo Alberto Cecchetti,
Satyabrata Kar, Kevin E. Quinn, Lorenzo Romagnani,
Marco Borghesi

International Research Centre for Experimental Physics,
School of Mathematics and Physics,
Queen's University, Belfast, UK

Outline

- Laser-Plasma interactions in the “relativistic” regime
- Laser-Accelerated Protons as a probe of Laser-Plasma interactions
- Proton probing-based investigations
  - ➔ Plasma expansion and sheath acceleration
  - ➔ Pulse self-channeling and coherent magnetic structures
  - ➔ Ultrafast charging dynamics
- Ultracold laser-produced plasmas: similarities, differences, present interest and challenges

Laser-Matter Interaction Scenario @ I=10^{20} W/cm^2

Electric field $$E = \sqrt{4\pi \frac{I}{c}} = 2.7 \times 10^{16}\ \mathrm{V/m} = 53 \frac{e}{r_{\mathrm{Bohr}}^2}$$ → **ultrafast ionization and plasma production**

Electron momentum $$p_{\mathrm{osc}} = \frac{eE}{\omega} = 8.5 m_e c\ @\ \lambda = 1\ \mu\mathrm{m}$$ → **electrons are strongly relativistic**

Radiation pressure $$P_{\mathrm{rad}} = \frac{I}{c} = 3.3 \times 10^{15}\ \mathrm{N/m^2}$$ → **radiation pressure dominates hydrodynamics**

Pulse duration may be
< 10 laser cycles
(e.g. 30 fs=3 x 10^{-14} s)
i.e the focused "laser beam" is a
light bullet

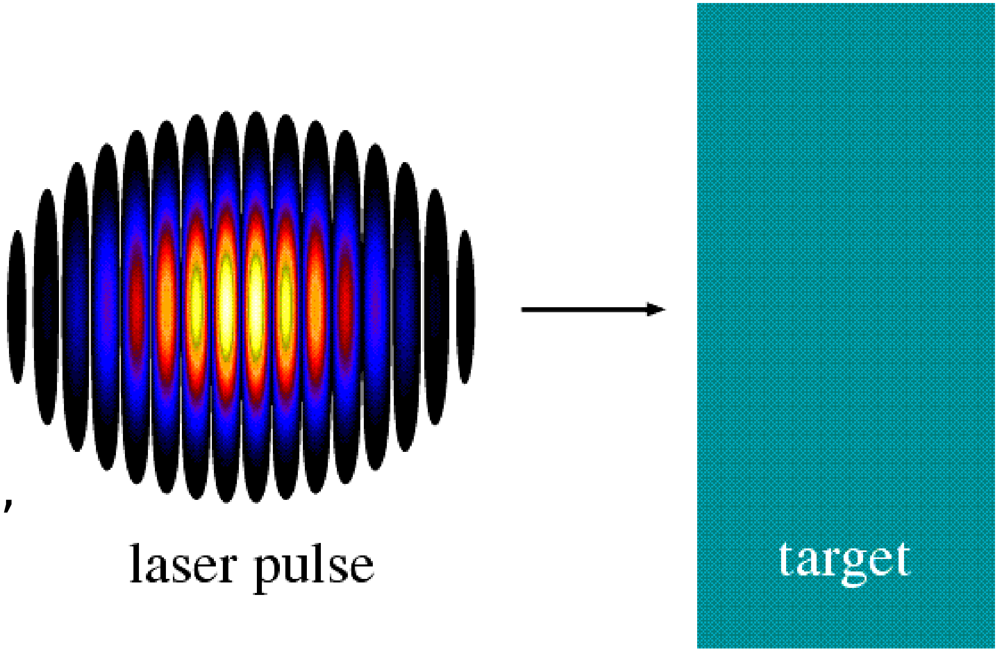

Related Definitions:
"*Extreme Light*", "*High Field Science*",
"*Relativistic Optics*",
"*High Energy Density Physics*" ...

G.Mourou, T.Tajima, S.V.Bulanov, Rev.Mod.Phys. **78** (2006) 309

“Fast” (relativistic) electron generation in solid targets

Forced oscillations of electrons across a sharp plasma interface *($L << \lambda$)* are strongly non-adiabatic and lead to energy absorption from the EM (laser) wave

As can be shown with a simple electrostatic model at each cycle electron bunches are ejected into the vacuum region and re-enter the plasma with high momentum (“vacuum heating”)
[Brunel, PRL **59** (1987) 52]

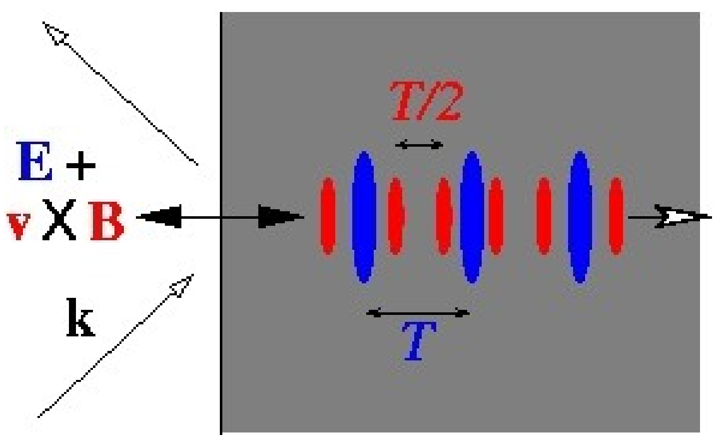

The $\mathbf{E}_{\perp}$ and **v**X**B** components drive electron bunches with different periodicity ($T=2\pi/\omega$ and $T/2$)

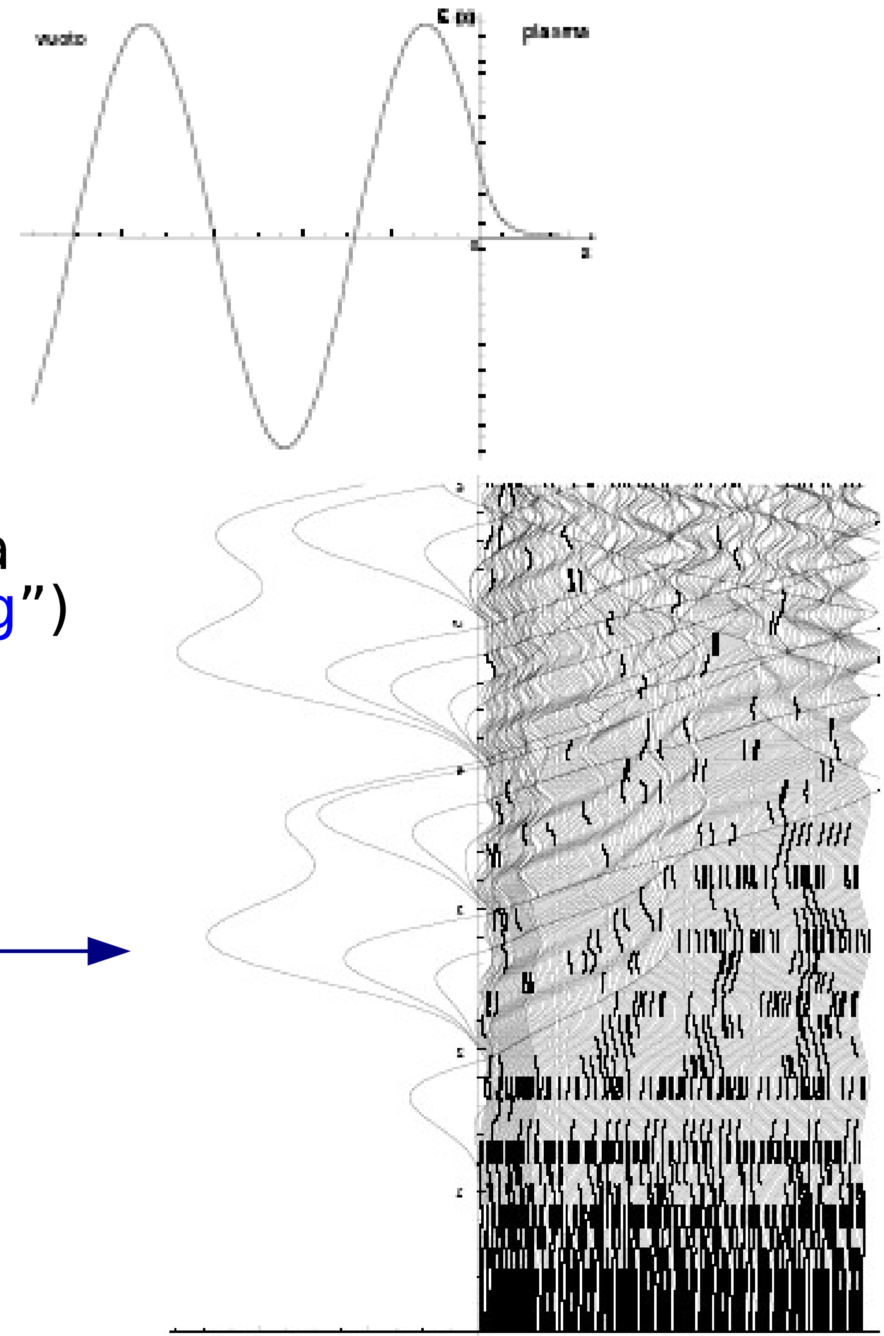

S. Tuveri, thesis, 2006

The discovery of MeV proton emission in superintense interaction with *metallic* targets

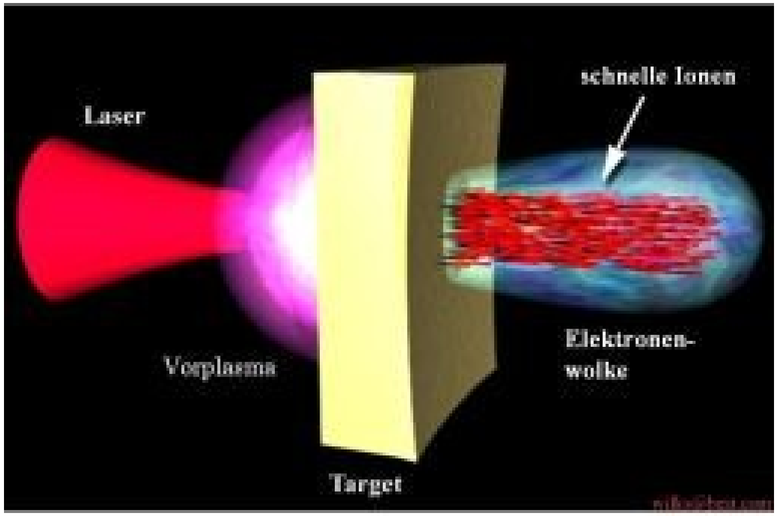

Reported in 2000
by three experimental groups

[Clark et al, PRL **84** (2000) 670;
Maksimchuk et al, *ibid.*, 4108;
Snavely et al, PRL **85** (2000) 2945 (*)]

Remarkable properties of the proton beam:

- **high number** (up to 10^{14})
- **good collimation**
- **ultra-low emittance** (4×10^{-3} mm mrad)
- maximum energy and efficiency observed (*):
  58 MeV , **12% of laser energy**
  @ $I = 3 \times 10^{20}$ W/cm^2

The discovery of MeV proton emission in superintense interaction with *metallic* targets

Reported in 2000
by three experimental groups

[Clark et al, PRL **84** (2000) 670;
Maksimchuk et al, *ibid.*, 4108;
Snavely et al, PRL **85** (2000) 2945 (*)]

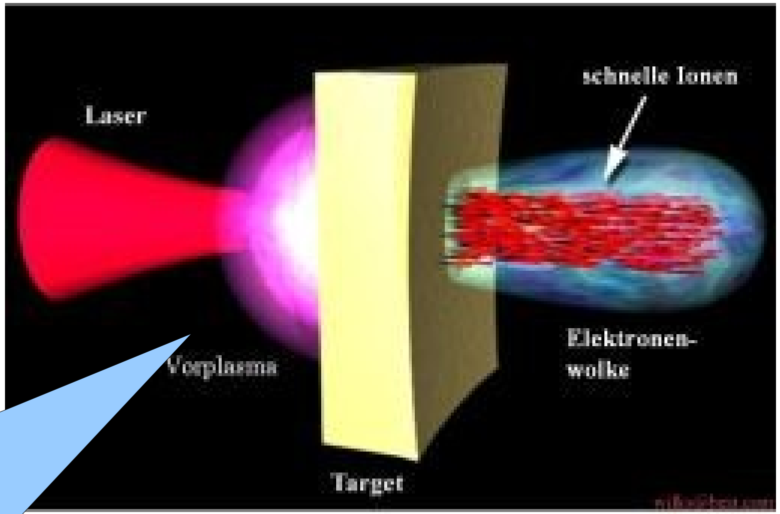

Rem
of th

er (up to 10^{14})
ation
ittance (4×10^{-3} mm mrad)
rgy and efficiency

% of laser energy
W/cm^2

Question: why protons

from *metallic* targets?

Answer: presence of a layer
of hydrocarbon or water
impurities on
the target surface

The discovery of MeV proton emission in superintense interaction with *metallic* targets

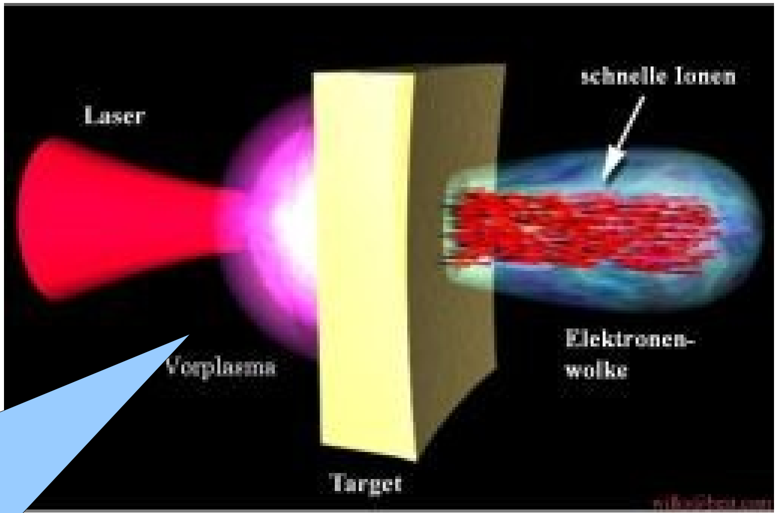

Reported in 2000
by three experimental groups

[Clark et al, PRL **84** (2000) 670;
Maksimchuk et al, *ibid.*, 4108;
Snavely et al, PRL **85** (2000) 2945 (*)]

More debated question: are protons coming from the *front* or from the *rear* side?

i.e. *what is the acceleration mechanism*?

Rem

of th

er (up to 10^{14})

ation

ittance (4 x 10^{-3} mm mrad)

rgy and efficiency

% of laser energy

W/cm^2

The “front vs rear side” debate

Clark et al: “It is likely that the protons originate from the front surface of the target and are bent by large magnetic fields which exist in the target interior.”

Maksimchuk et al: “The protons [...] appear to originate from impurities on the front side of the target [...] The maximum proton energy can be explained by the charge-separation electrostatic-field acceleration due to *vacuum heating*.”

Snavely et al: “We have concluded that light pressure effects at the front surface focal spot on the target could not generate the observed ions because of the clear evidence that the protons are emitted perpendicular to the rear surface(s) of the target.”

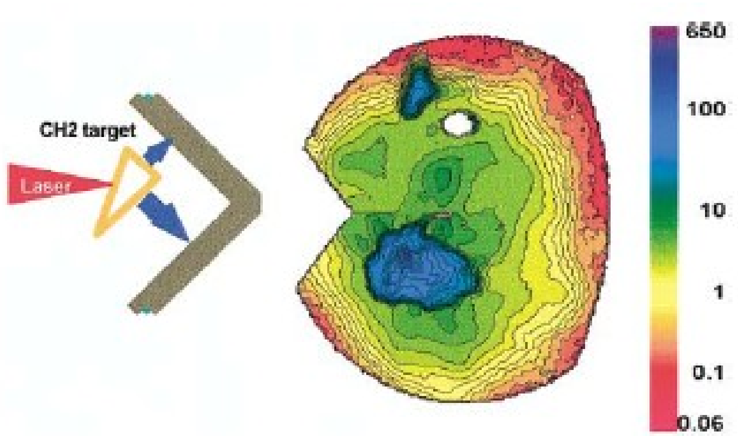

FIG. 4 (color). Contours of dose in krads as a function of angle recorded on a RC film through 300 μm Ta (proton $E >$ 18 MeV). The image clearly shows two proton beams, the larger from the major face and the smaller from the minor face of the wedge.

The Target Normal Sheath Acceleration model

Physical mechanism:
proton acceleration by the space-charge electric field generated by “fast” electrons escaping from the target

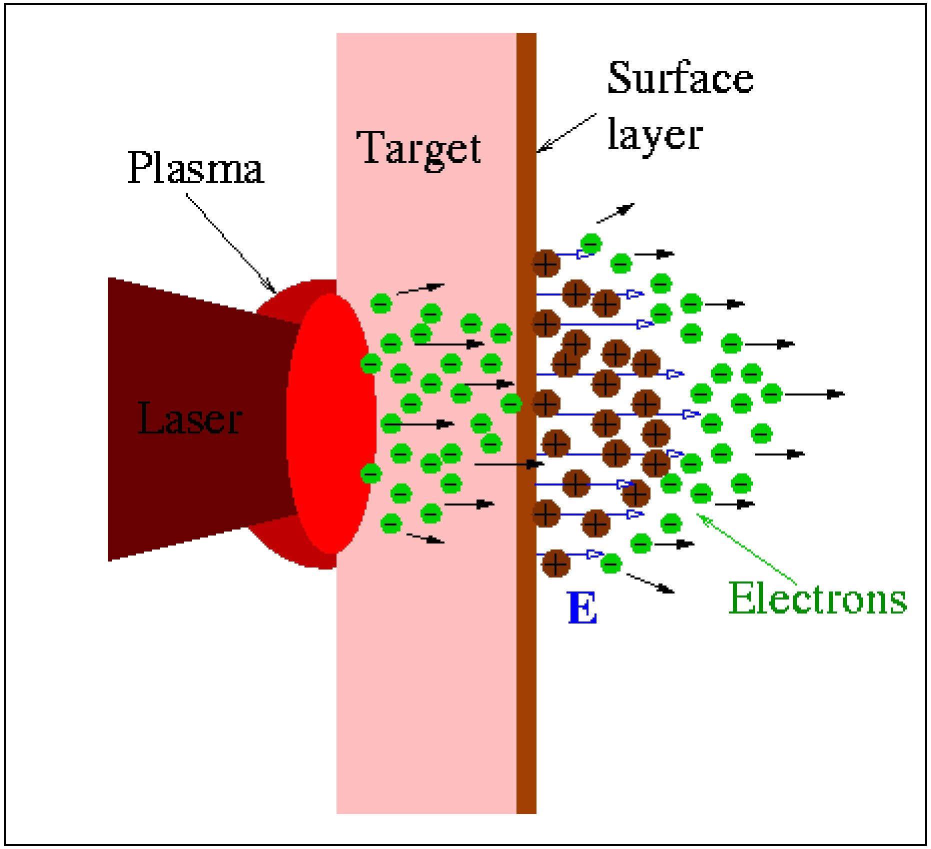

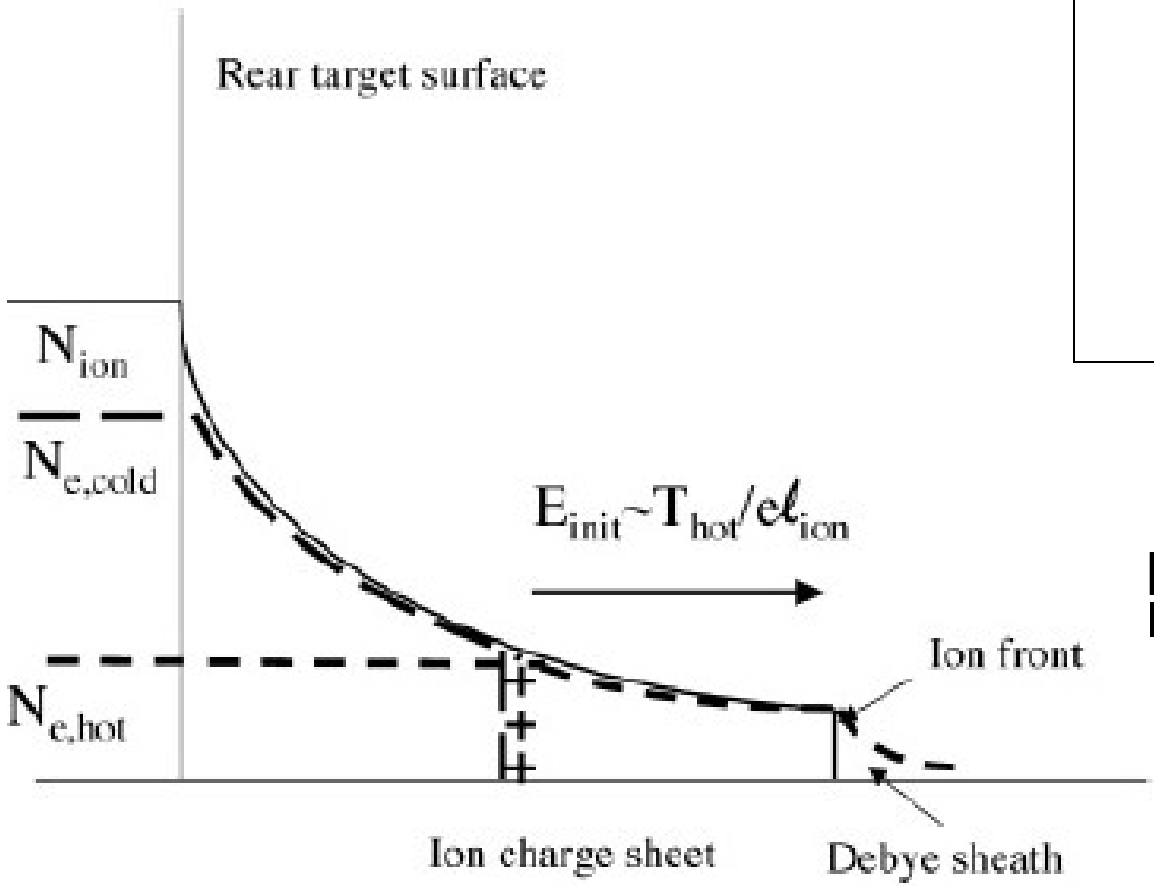

[S. Wilks et al,
Phys. Plasmas **8** (2001) 542]

Modeling of sheath acceleration: the classic problem of plasma expansion in vacuum

Analytical approach:
- electrostatic
- fluid ions
- electrons in Boltzmann equilibrium
- electron temperature T_e and density n_e as input parameters

$$n_e = n_0 \exp\left(\frac{e\Phi}{k_B T_e}\right), \qquad \nabla^2\Phi = Zen_i - en_e$$

$$\frac{d\mathbf{v}_i}{dt} = \frac{Ze}{Am_p}\mathbf{E} = -\frac{Ze}{Am_p}\boldsymbol{\nabla}\Phi, \qquad \partial_t n_i = -\boldsymbol{\nabla}\cdot(n_i\mathbf{v}_i)$$

"Mora's formula" from isothermal, semi-infinite slab model
[P.Mora, PRL **90** (2003) 185002]

$$v_i \simeq 2c_s \ln\left(\omega_{pi}t_p + \sqrt{\omega_{pi}^2 t_p^2 + 1}\right)$$

$$c_s = \sqrt{\frac{Zk_BT_e}{Am_p}}, \qquad \omega_{pi} = \sqrt{\frac{4\pi Zn_ie^2}{Am_p}}$$

- diverges with time (infinite energy available!)
- "corrected" assuming finite acceleration time t_p
[J.Fuchs et al, Nature Phys. **2** (2005) 48]

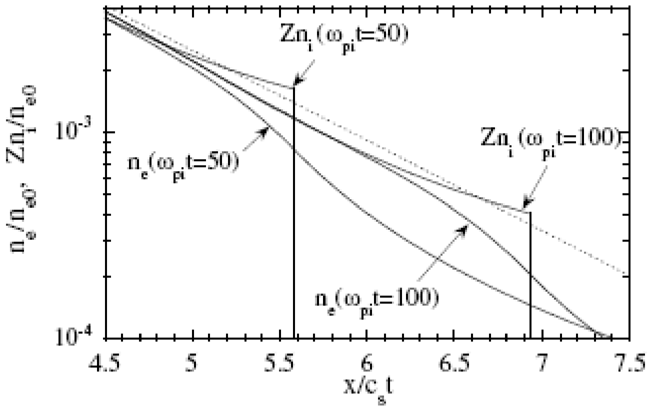

Modeling of sheath acceleration: the classic problem of plasma expansion in vacuum

Analytical approach:

$$n_e = n_0 \exp\left(\frac{e\Phi}{k_B T_e}\right), \qquad \nabla^2\Phi = Zen_i - en_e$$

$$\frac{d\mathbf{v}_i}{dt} = \frac{Ze}{Am_p}\mathbf{E} = -\frac{Ze}{Am_p}\boldsymbol{\nabla}\Phi, \qquad \partial_t n_i = -\boldsymbol{\nabla}\cdot(n_i\mathbf{v}_i)$$

- electrostatic
- fluid ions
- electrons in Boltzmann equilibrium
- "fast" electron temperature and density as input parameters
- **thin slab** to account for **finite energy**

Excellent agreement with numerical PIC results (numerical solution of the Vlasov kinetic equation):

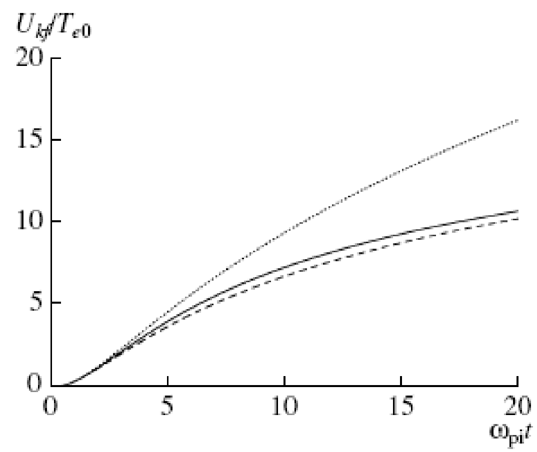

Fig. 3. The kinetic energy acquired by the fastest ion during the expansion of a slab of total thickness $2a = 40$ as predicted by the numerical simulations (solid line), by the analytical model (dashed line), and by the semi-infinite model [11] (dotted line).

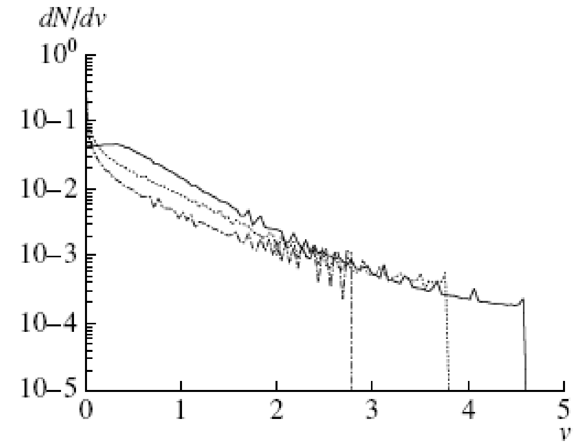

Fig. 4. Ion velocity spectrum at $\tau = 5$ (dashed line), $\tau = 10$ (dotted line), and $\tau = 20$ (solid line). The initial slab total size is $2a = 40$ and v is normalized to the initial sound speed.

S.Betti, F.Ceccherini, F.Cornolti, F.Pegoraro, Plasma Phys. Control. Fusion **47** (2005) 521;
F.Ceccherini, S.Betti, F.Cornolti, F.Pegoraro, Laser Physics **16** (2006) 1

Basis of theoretical and numerical modeling

"Plasma physics is just waiting for bigger computers"

Vlasov-Maxwell system for *collisionless, classical* plasmas: kinetic equations are coupled to EM fields

$$\frac{df_a}{dt}(\mathbf{x},\mathbf{p},t) = \frac{\partial f_a}{\partial t} + \dot{\mathbf{x}}_a \frac{\partial f_a}{\partial \mathbf{x}} + \dot{\mathbf{p}}_a \frac{\partial f_a}{\partial \mathbf{p}} = 0, \quad a = (e,i)$$

$$\dot{\mathbf{p}}_a = q_a(\mathbf{E} + \mathbf{v} \times \mathbf{B}), \qquad \dot{\mathbf{x}}_a = \frac{\mathbf{p}_a}{m_a \gamma_a},$$

$$\rho(\mathbf{x},t) = \sum_{a=e,i} q_a \int d^3p f_a, \qquad \mathbf{J}(\mathbf{x},t) = \sum_{a=e,i} q_a \int d^3p \mathbf{v} f_a,$$

$$\nabla \cdot \mathbf{E} = \rho, \qquad \nabla \cdot \mathbf{B} = 0, \qquad \nabla \times \mathbf{E} = -\partial_t \mathbf{B}, \qquad \nabla \times \mathbf{B} = \mathbf{J} + \partial_t \mathbf{E}$$

Mostly used numerical approach: particle-in-cell (PIC) method
[Birdsall & Langdon, *Plasma Physics via Computer Simulation* (IOP, 1991)]

3D numerical simulations of "realistic" experimental conditions is most of the times beyond present-day supercomputing power

Models are needed to interpretate experiments and unfold the underlying physics

How to diagnose the electric fields directly?
Idea: use the protons as a probe

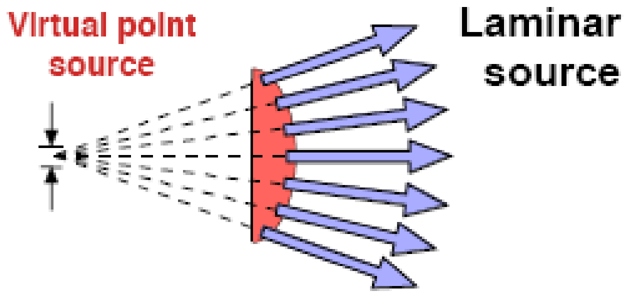

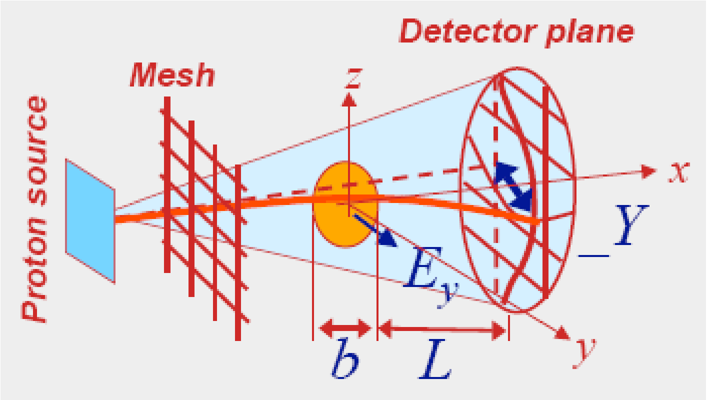

Due to high laminarity the proton beam has **imaging properties**

The short duration of the proton burst allows **picosecond temporal resolution**

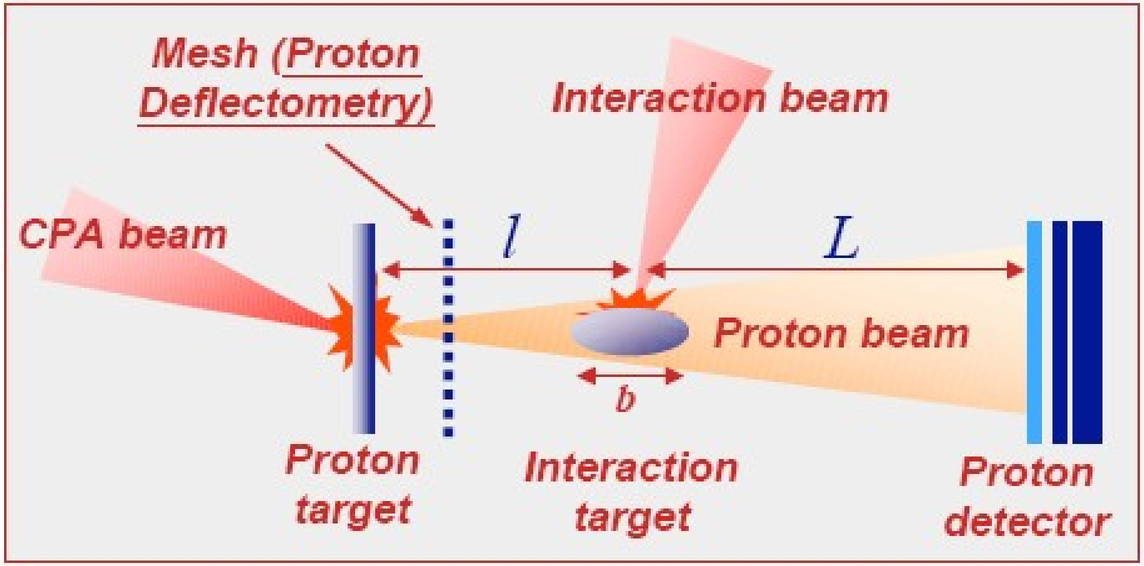

Borghesi et al, Phys.Plasmas **9** (2002) 2214
Borghesi et al, Phys.Rev.Lett. **92** (2004) 055003
Cowan et al, Phys.Rev.Lett. **92** (2004) 204851

Protons of a given energy will cross the probed object at a particular time.
An energy-resolving detector (e.g. Radiochromic Film) thus provides **multiframe capability**

In a laser-plasma experiment the proton probe is easily **synchronized with the interaction**

Energy resolving allows temporal resolution

Use of RadioChromic Film (RCF) stack as a detector allows single-shot, spatial and **energy** resolution of the proton beam

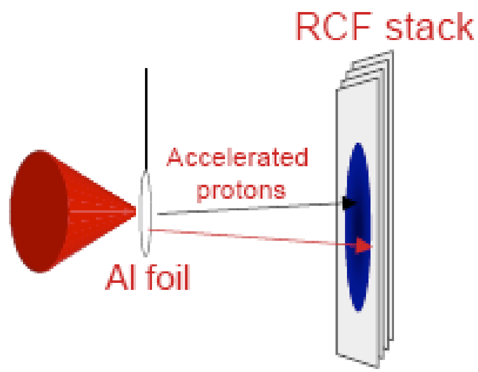

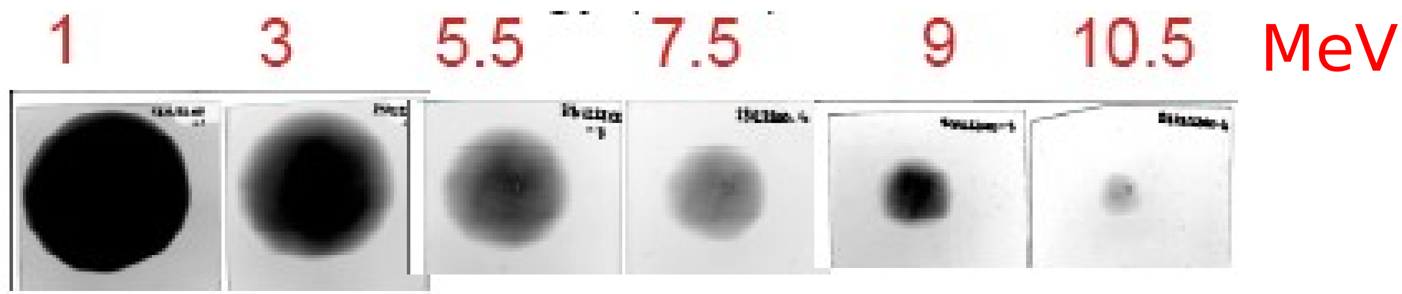

Typical data example

(taken at the LULI 100 TW facility, École Polytechnique, Palaiseau, France)

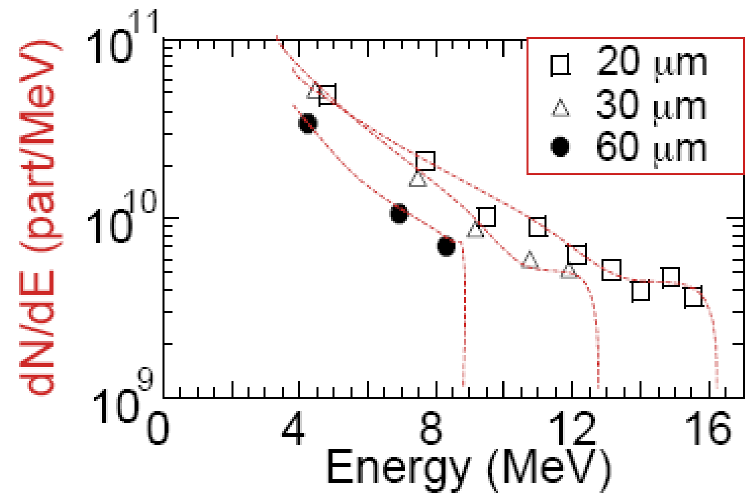

RCF energy selection capability is a consequence of Bragg peak deposition

Energy resolving allows temporal resolution

Use of RadioChromic Film (RCF) stack as a detector allows single-shot, spatial and **energy** resolution of the proton beam

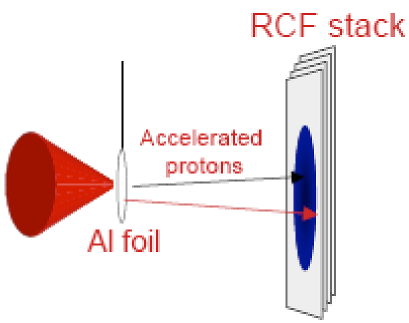

1 3 5.5 7.5 9 10.5 MeV

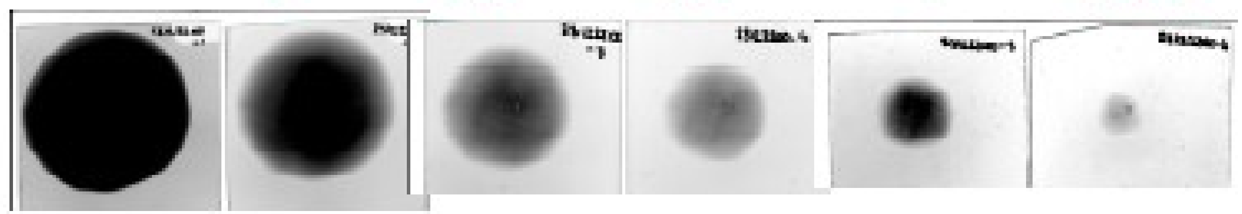

72 42 31 26 24 22 ps

In a time-of-flight arrangement protons of different energies cross the object at different times: imaging of transient objects possible

RCF energy bandwidth allows picosecond resolution

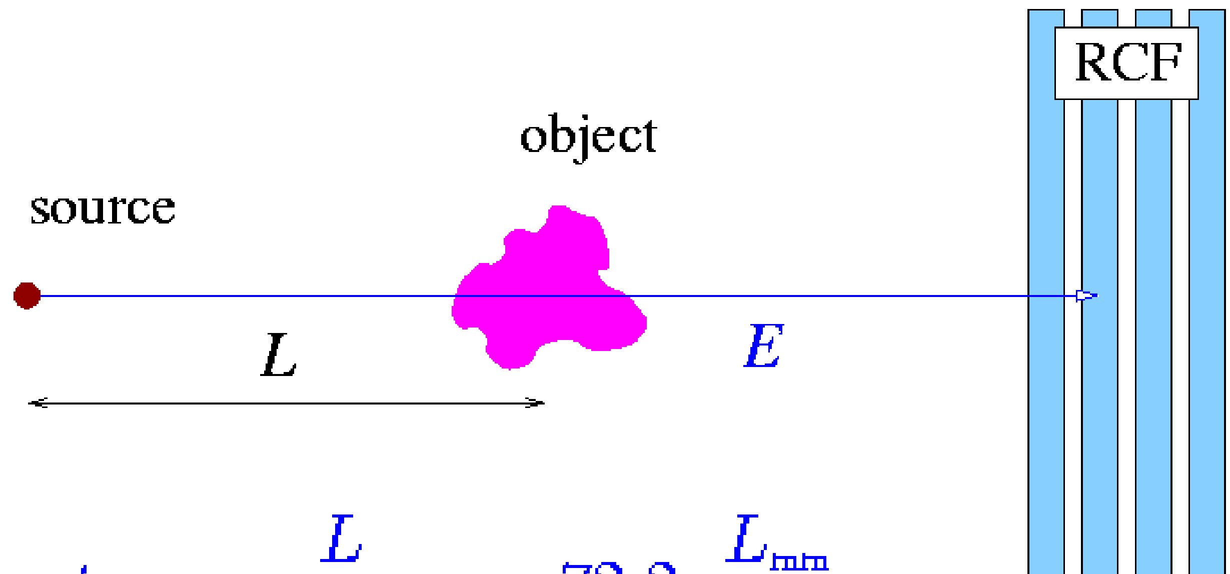

$$t_p = \frac{L}{\sqrt{2E/m_p}} = 72.2\frac{L_{\mathrm{mm}}}{\sqrt{E_{\mathrm{MeV}}}}\mathrm{ps}$$

Using protons to detect EM fields

A proton crossing an EM field distribution acquires a transverse velocity $\delta\ \mathbf{v}$

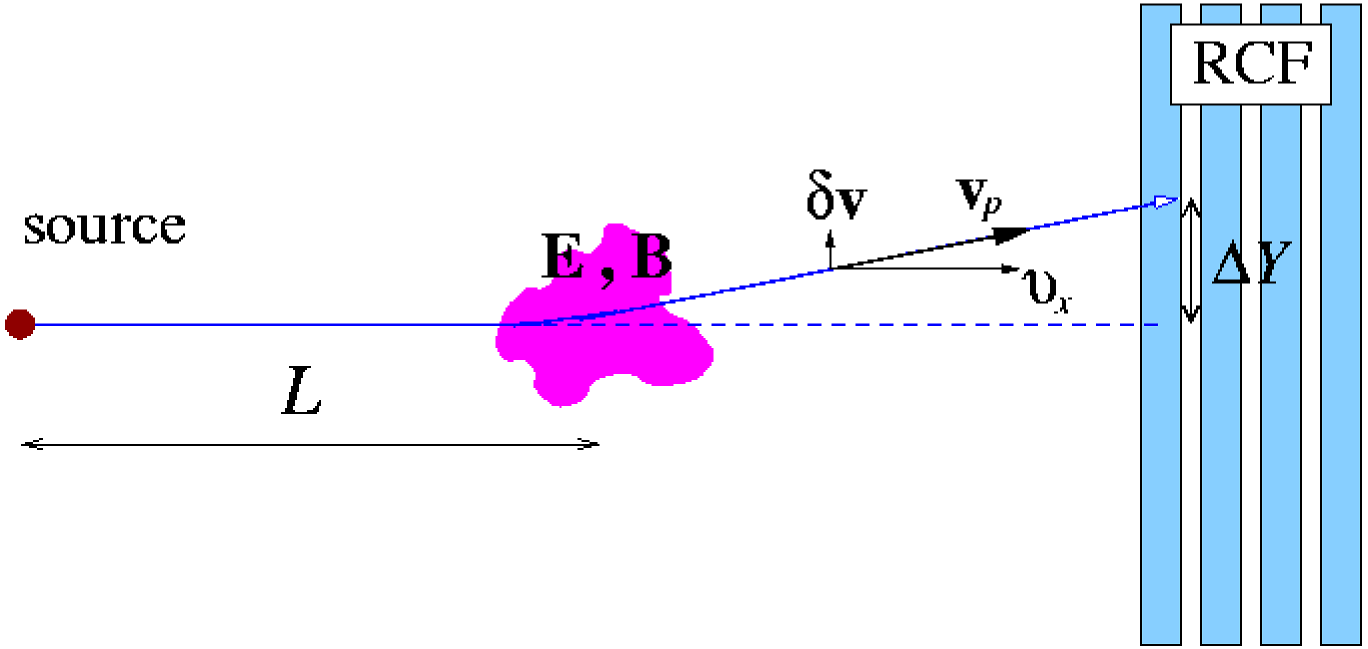

$$\delta\mathbf{v} = \frac{e}{m_p}\int(\mathbf{E}+\mathbf{v}_p\times\mathbf{B})\,dt$$

For *weak* deflections (1st order Born approximation)

$$v_x = \frac{dx}{dt} \simeq v_p \quad \rightarrow \quad \delta Y = |\delta\mathbf{v}_\perp|\Delta t \simeq \frac{eL}{2\mathcal{E}_p}\int(\mathbf{E}+\mathbf{v}_p\times\mathbf{B})_\perp\,dx$$

Concept: estimate $\mathbf{E}$ (and/or $\mathbf{B}$) from the measurement of $\Delta\ Y$

Proton "Deflectometry"

The proton deflection $\Delta\ Y$ can be measured directly by the deformation of the imprint of a stopping mesh

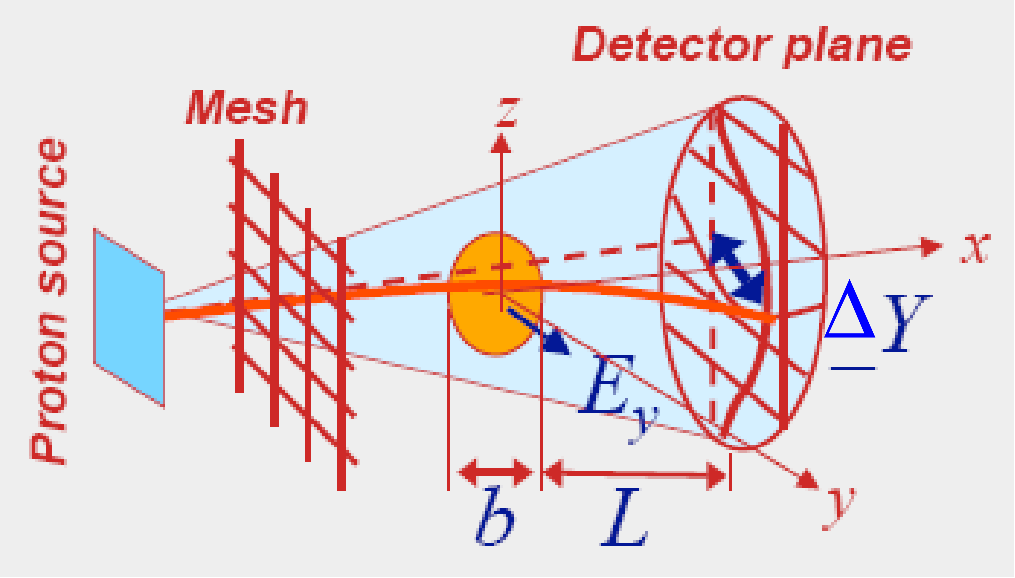

Assuming that only E contributes we estimate the average field as

$$\langle \mathbf{E} \rangle \simeq \frac{1}{b} \int_{-b/2}^{+b/2} \mathbf{E}_{\perp} dx \simeq \frac{2\mathcal{E}_p}{eLb} \Delta Y$$

Proton "Imaging"

When fields gradients are present deflections produce a modulation $\delta\ n$ in the proton density n_p on the detector plane:

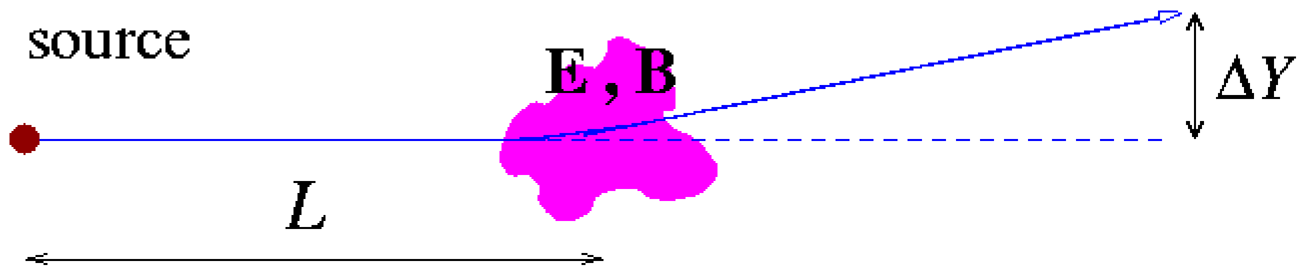

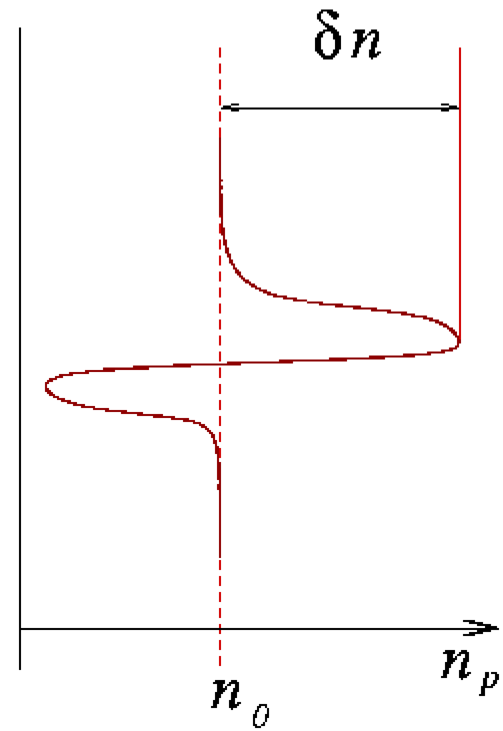

The observed modulation $\delta\ n$ is proportional to the line integral of "source" terms

(M : geometrical magnification)

$$\frac{\delta n}{n_0} \simeq -\frac{1}{M}\boldsymbol{\nabla}_{\perp}\cdot\Delta\mathbf{Y} \simeq -\frac{2\pi e L b}{\mathcal{E}_p M}\int_{-b/2}^{+b/2}\left(\rho - \frac{1}{c^2}\mathbf{v}_p\cdot\mathbf{J}\right)dx$$

Modeling of “proton probing experiments”

Interpretation of proton diagnostic data usually occurs through three steps:

1. Find a model (analytical and/or numerical) for the electric field $\mathbf{E}(x,t)$ [and/or the magnetic field $\mathbf{B}(x,t)$]

   - frequent need to bridge the gap between temporal scales or dimensionality of laser-plasma “ab initio” simulations (particle-in-cell method) and those of the experiment:

   fs $\rightarrow$ ps , 2D $\rightarrow$ 3D

2. Simulate the proton diagnostic via particle tracing simulations with $\mathbf{E}(x,t)$ [and/or $\mathbf{B}(x,t)$] as input

3. Compare simulated proton images with experimental ones

Detection of Proton-Accelerating Sheath Fields

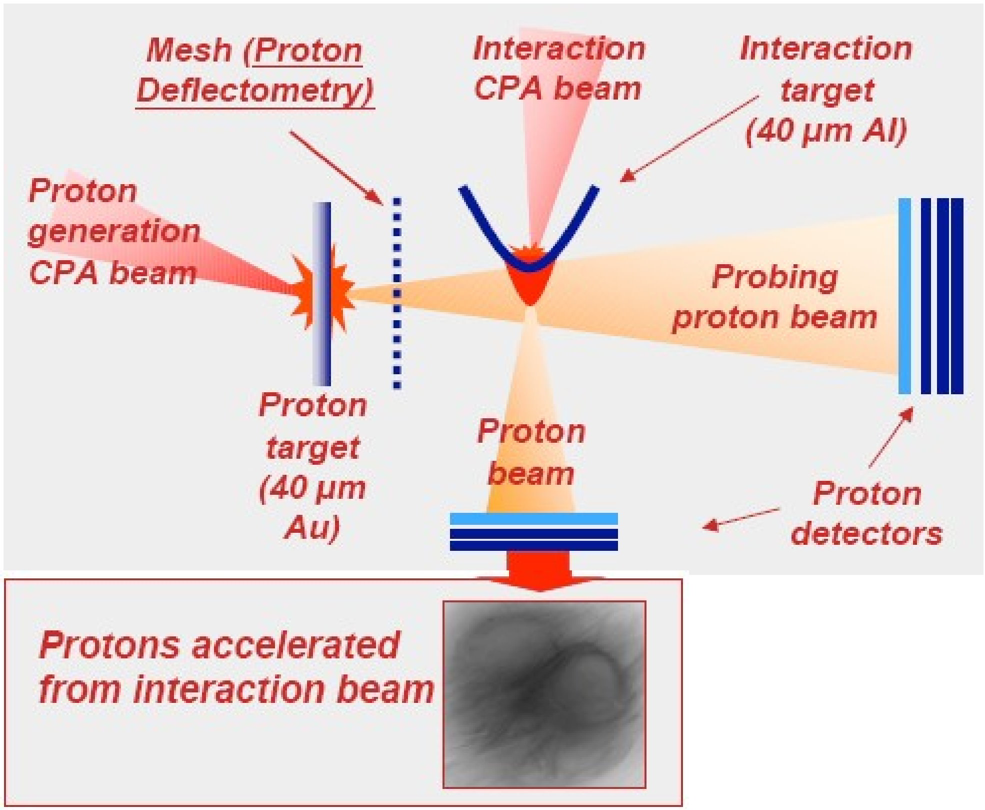

Goal: study of TNSA mechanism for ion acceleration
by the direct detection of related space-charge electric field

Technique: use a second proton beam as a transverse probe

Detection of Proton-Accelerating Sheath Fields

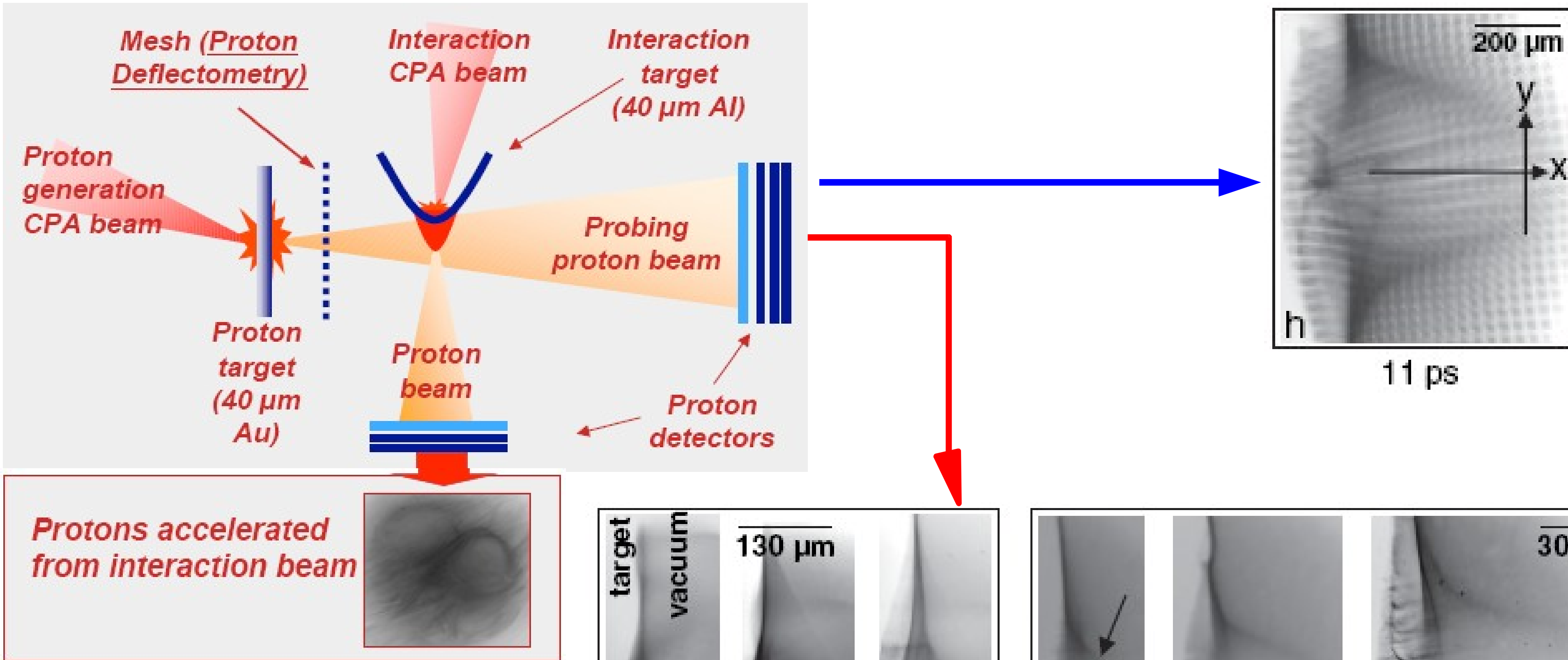

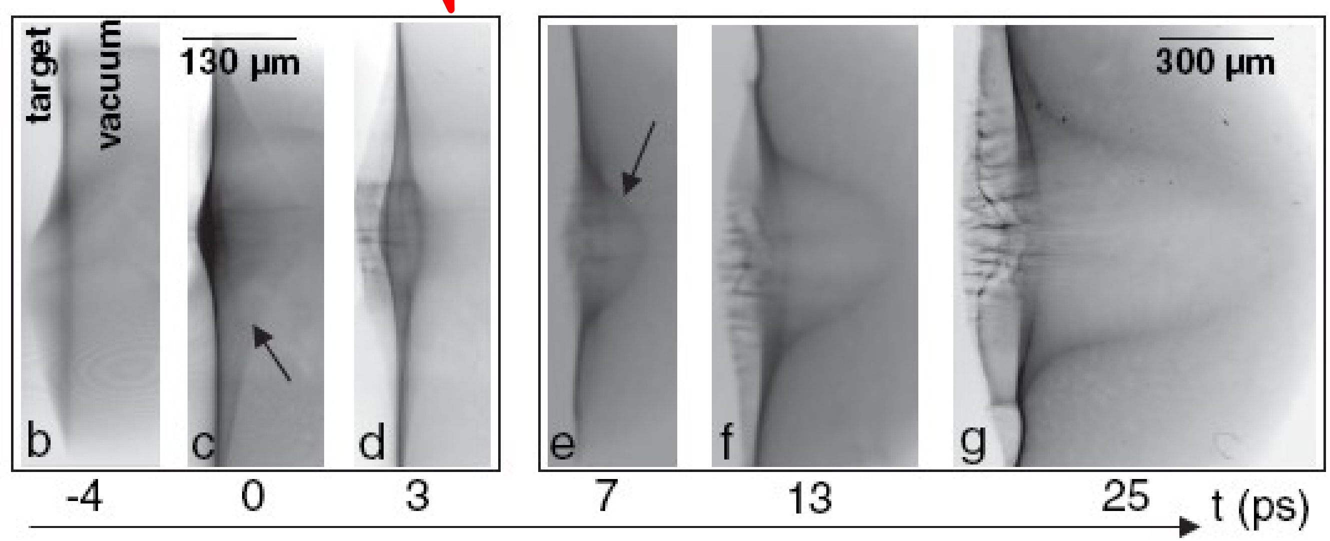

Expanding,
bell-shaped front
observed in proton
images and
deflectograms

L. Romagnani, J. Fuchs, M. Borghesi, P. Antici, P. Audebert, F. Ceccherini, T. Cowan, T. Grismayer, S. Kar, A. Macchi, P. Mora, G. Pretzler, A. Schiavi, T. Toncian, O. Willi, Phys. Rev. Lett. **95** (2005) 195001

Experimental detection of sheath fields using the proton diagnostic

Experimental results have been compared with PIC simulations using the plasma expansion model.

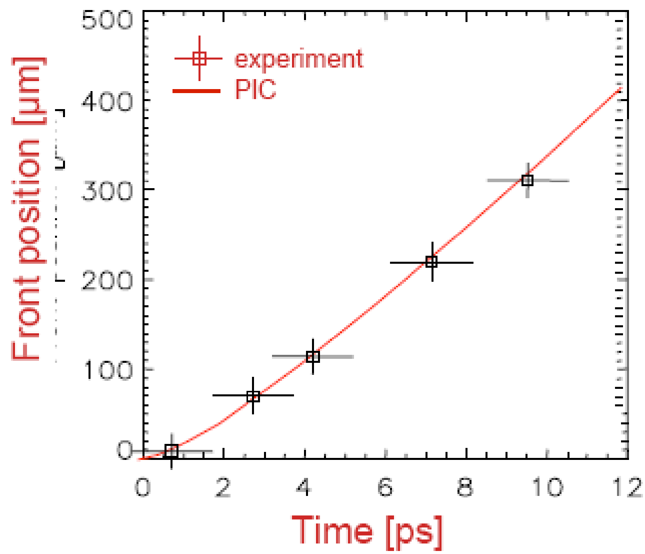

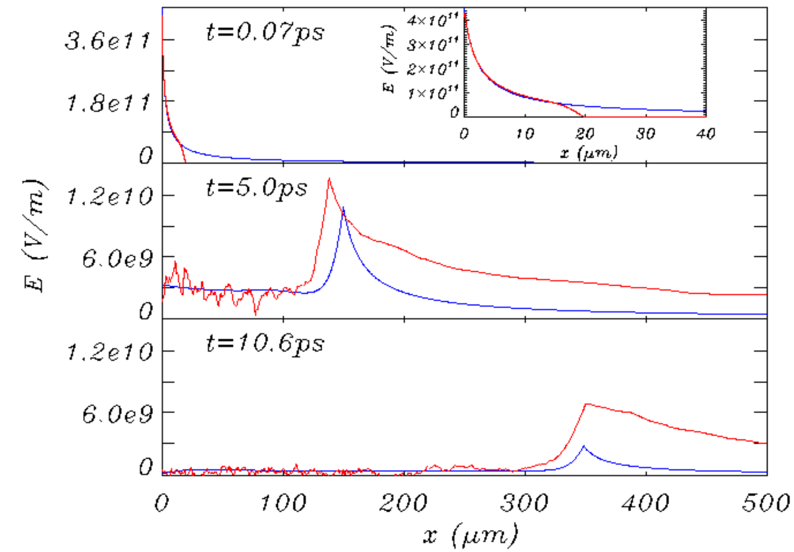

Particle tracing simulations of proton deflection in the PIC fields (plus an “heuristic” modeling of the 2D expansion) fit well experimental images and deflectrograms

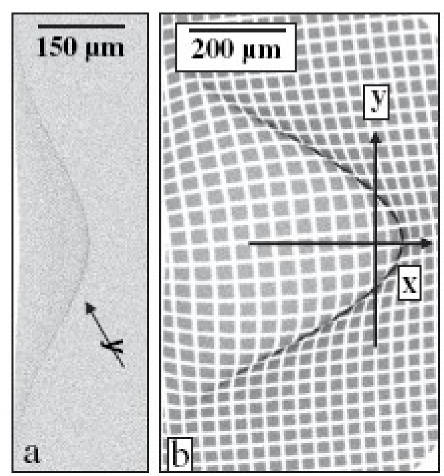

Comparison of fluid and kinetic (PIC) results show the importance of **non-**equilibrium, **kinetic** and **non-Maxwellian** effects in the plasma expansion

L. Romagnani, J. Fuchs, M. Borghesi, P. Antici, P. Audebert, F. Ceccherini, T. Cowan, T. Grismayer, S. Kar, A. Macchi, P. Mora, G. Pretzler, A. Schiavi, T. Toncian, O. Willi, Phys. Rev. Lett. **95** (2005) 195001

Study of charge-displacement self-channeling

A superintense laser pulse propagating in a low-density plasma (produced in a gas jet) undergoes self-focusing and channeling due to both relativistic effects and radial plasma expulsion by radiation pressure.

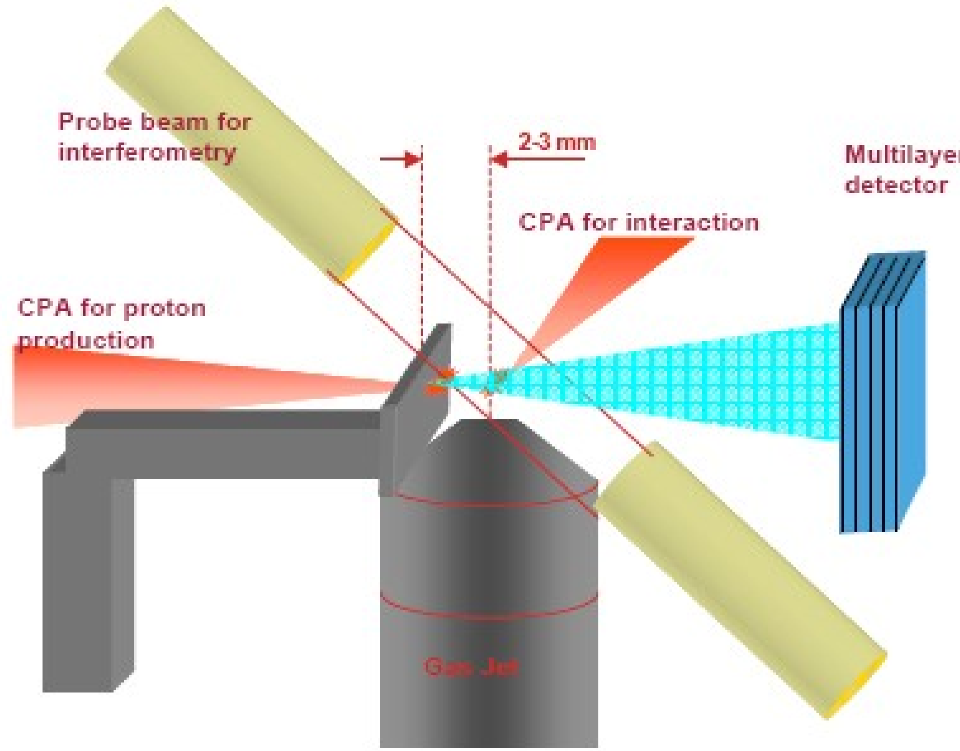

For a transient stage the channel is charged since electrons are expelled first.

Proton probing along the direction perpendicular to propagation has been used to study this effect

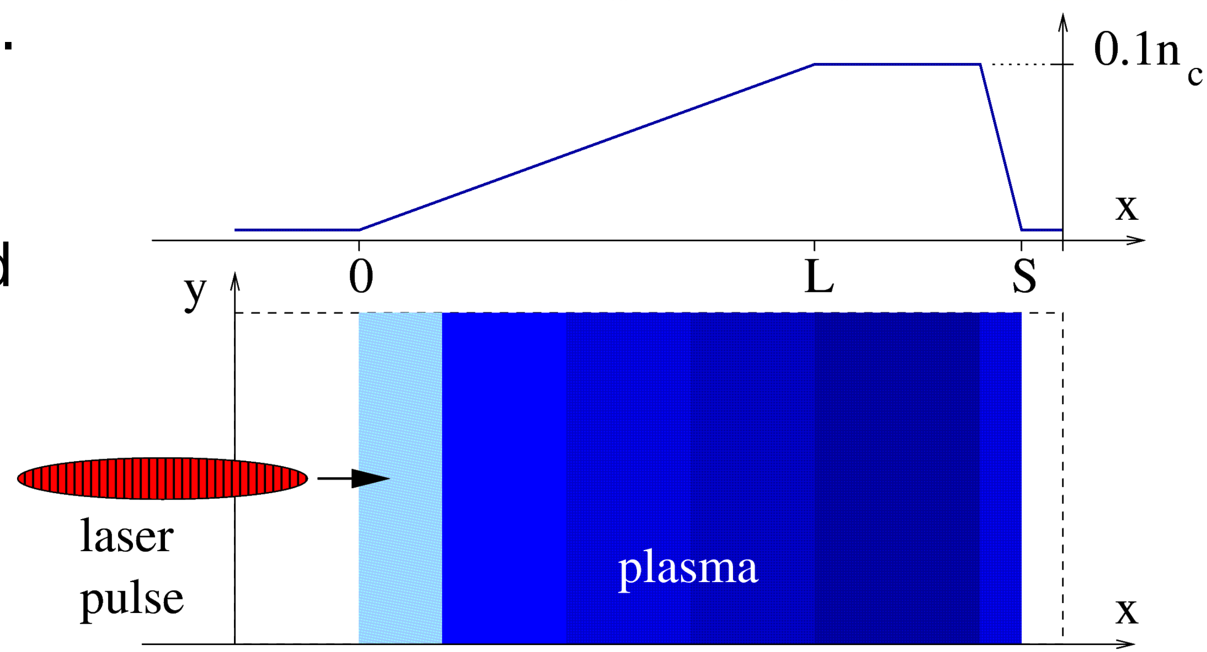

Proton images of charged channel evolution

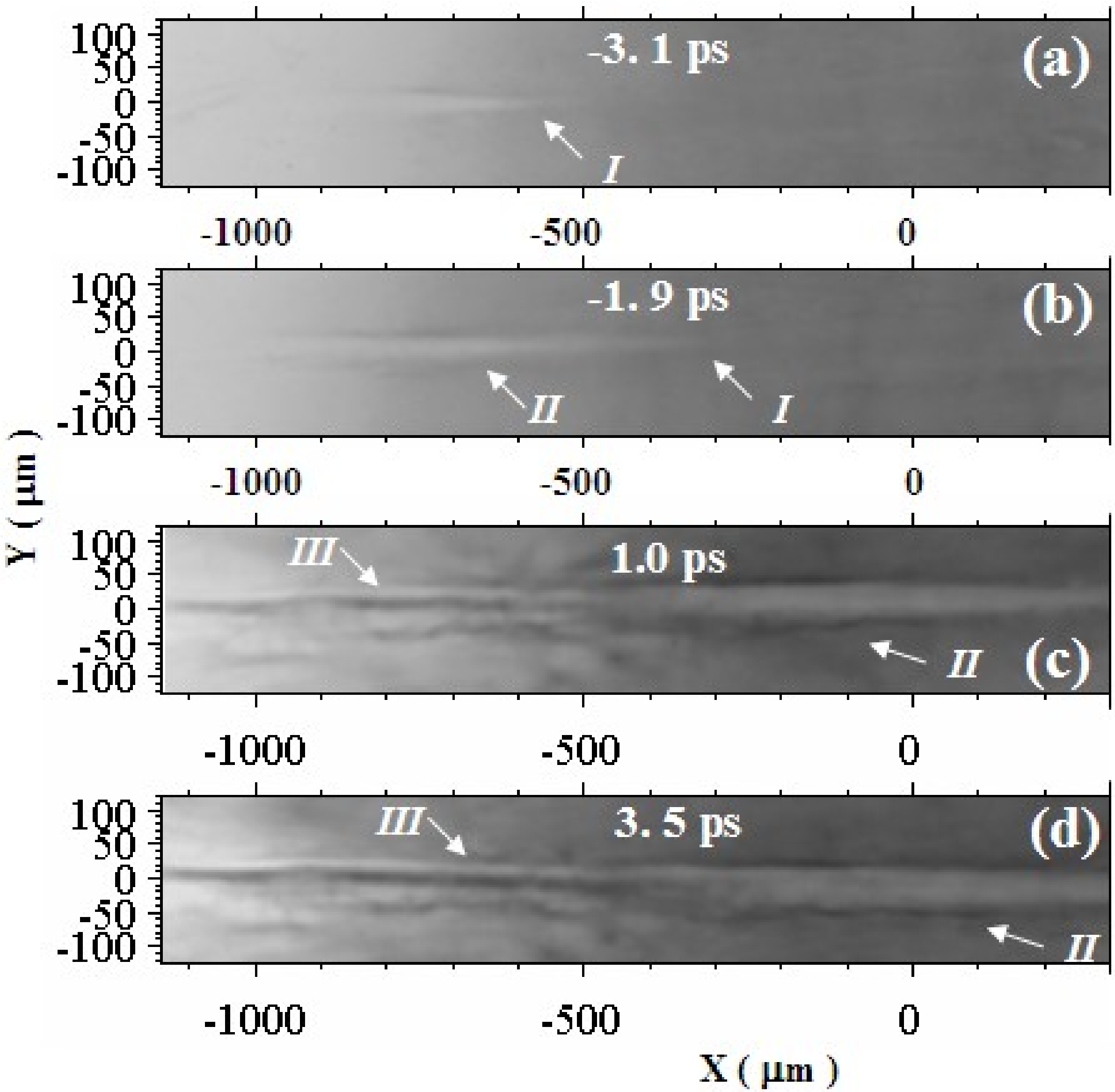

Early times (during the laser pulse) propagating "white" channel front indicates electron expulsion from the axis

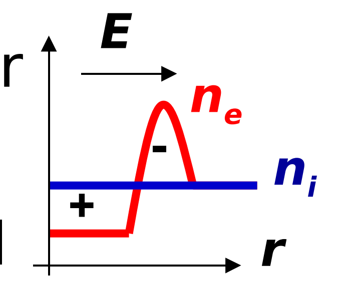

Late times (after the laser pulse) "black" line on axis indicates field inversion at some location

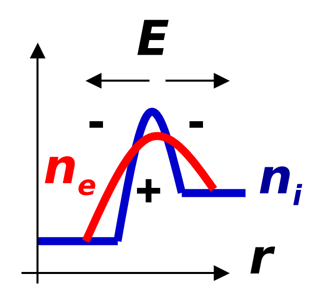

S.Kar, M.Borghesi, C.A.Cecchetti, L.Romagnani, F.Ceccherini, T.V.Lyseikina, A. Macchi, R.Jung, J.Osterholz, O.Willi, M.Galimberti, L.A.Gizzi, A.Schiavi, R.Heathcote, New J. Physics **9**, 402 (2007)

Channel front propagation speed

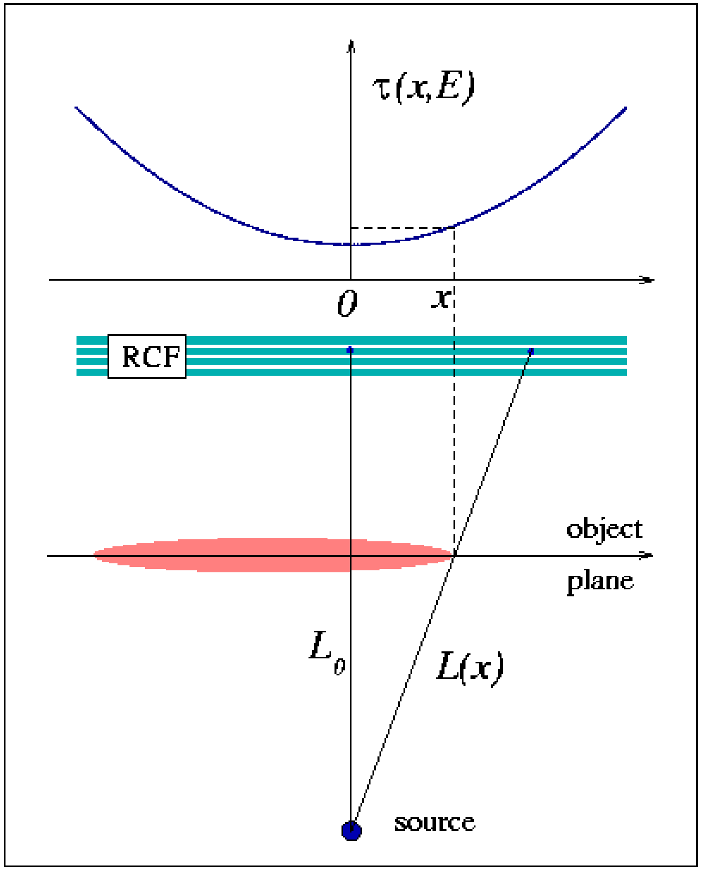

Due to the divergence of the proton beam the "probing time" depends on angle (i.e. on the position on the object plane)

$$\tau(x, E) = t_0(E) + \frac{L_0}{\sqrt{2E/m_p}}\left(\sqrt{1 + x^2/L_0^2} - 1\right)$$

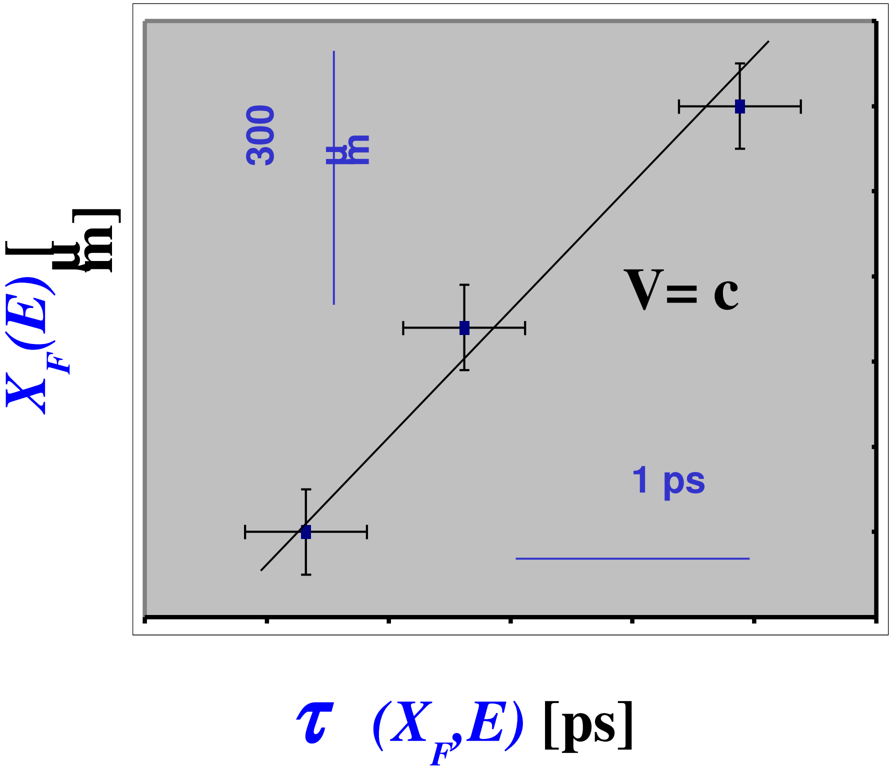

Plotting the channel front displacement $X_F(E)$ *vs.* the probing time $\tau\ (X_F,E)$ we obtain the front propagation speed $V \sim c$

2D PIC simulations show “radial” field dynamics

Laser

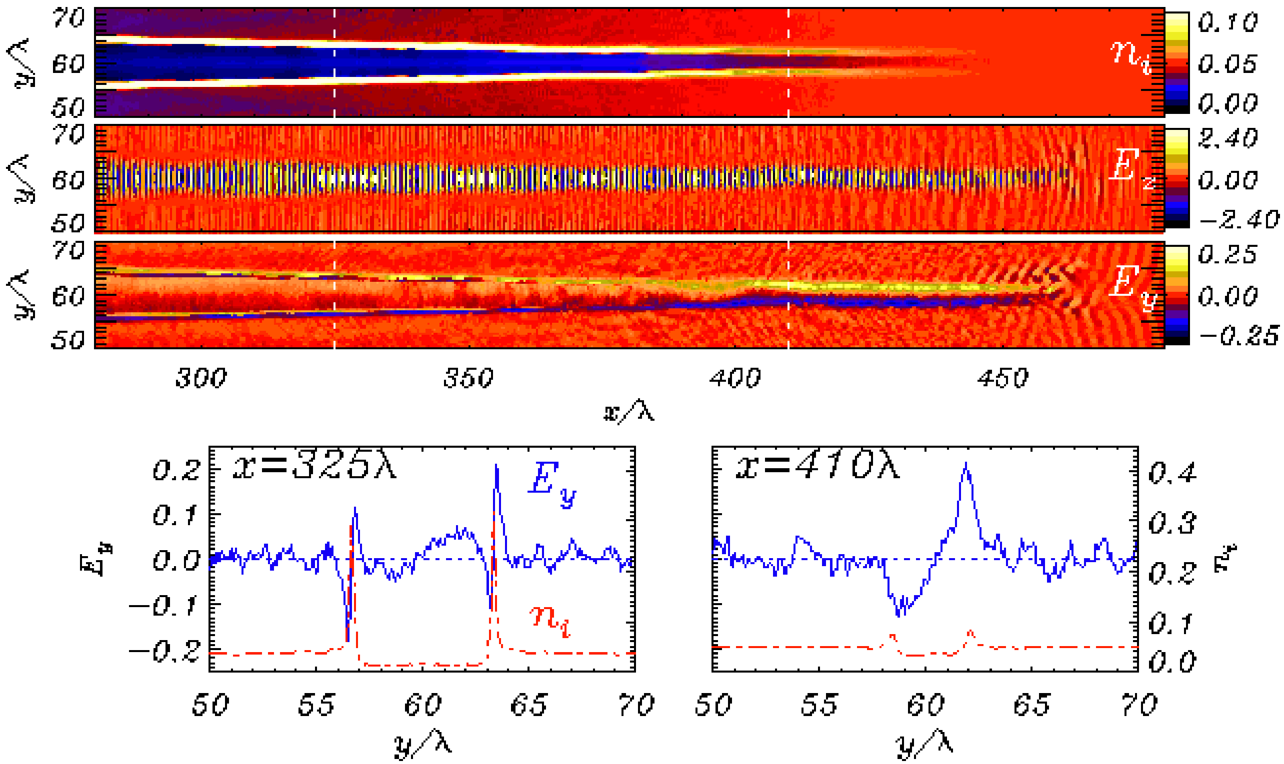

Two ambipolar fronts of E_y appear in the trailing edge of the channel; “negative” part can produce “black line” in proton images

Outward-directed radial field E_y due to electron expulsion from axis

EM component E_z reveals self-focusing

S.Kar, M.Borghesi, C.A.Cecchetti, L.Romagnani, F.Ceccherini, T.V.Lyseikina, A. Macchi, R.Jung, J.Osterholz, O.Willi, M.Galimberti, L.A.Gizzi, A.Schiavi, R.Heathcote, New J. Physics **9**, 402 (2007)

Ponderomotive model of self-channeling

Assumptions:
- cylindrical symmetry
- non-evolving laser pulse
- electrostatic approximation

Solution based on kinetic PIC model

$$
\begin{aligned}
m_e dv_e/dt &= -eE_r - m_e c^2 \partial_r \sqrt{1+a^2} \\
a = a(x,r,t) &= a_0 e^{-r^2/r_0^2 - (x-ct)^2/c^2\tau^2} \\
m_i dv_i/dt &= ZeE_r \\
\frac{1}{r}\partial_r (r \cdot E_r) &= 4\pi e (Zn_i - n_e)
\end{aligned}
$$

Particle tracing simulations using $\mathbf{E}$ from PIC model well reproduce experimental features

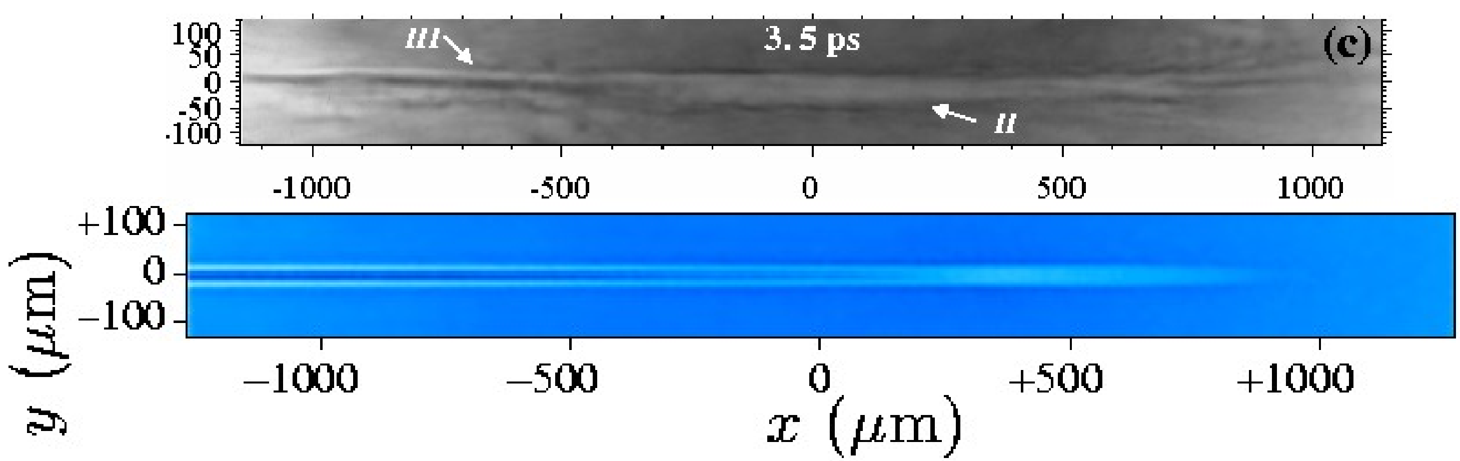

S.Kar, M.Borghesi, C.A.Cecchetti, L.Romagnani, F.Ceccherini, T.V.Lyseikina, A. Macchi, R.Jung, J.Osterholz, O.Willi, M.Galimberti, L.A.Gizzi, A.Schiavi, R.Heathcote, New J. Physics **9**, 402 (2007)

Ponderomotive model of self-channeling

Assumptions:
- cylindrical symmetry
- non-evolving laser pulse
- electrostatic approximation

Solution based on kinetic PIC model

$$
\begin{aligned}
m_e dv_e/dt &= -eE_r - m_e c^2 \partial_r \sqrt{1+a^2} \\
a = a(x,r,t) &= a_0 e^{-r^2/r_0^2-(x-ct)^2/c^2\tau^2} \\
m_i dv_i/dt &= ZeE_r \\
\frac{1}{r}\partial_r(r \cdot E_r) &= 4\pi e(Zn_i - n_e)
\end{aligned}
$$

The late ambipolar field appears after the vanishing of the early field ("echo" effect) due to hydrodynamical breaking in the ion density profile causing strong electron heating

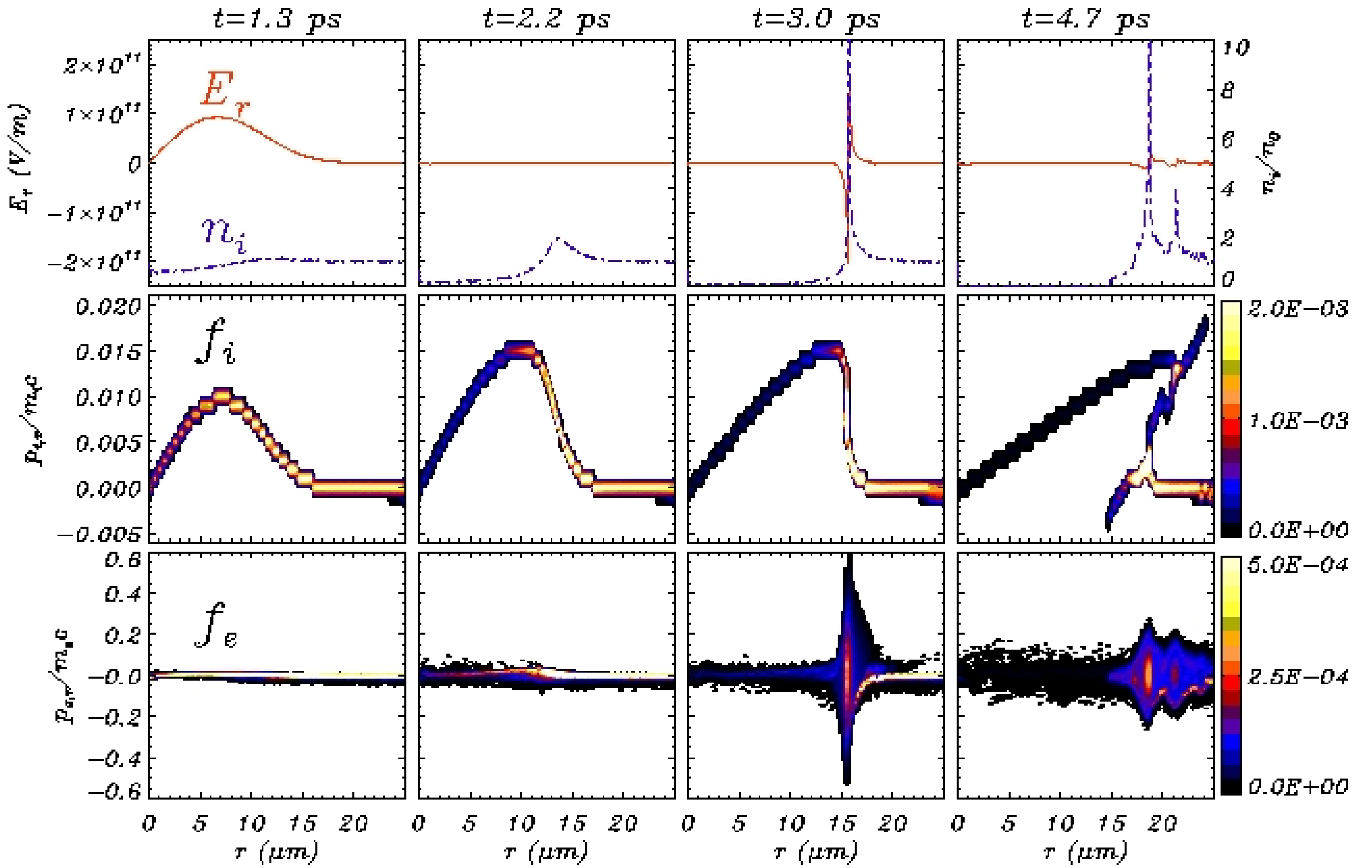

A. Macchi, F.Ceccherini, F. Cornolti, S.Kar, M.Borghesi, PPCF **51** (2009) 024005

Coherent field structures in 2D PIC simulation

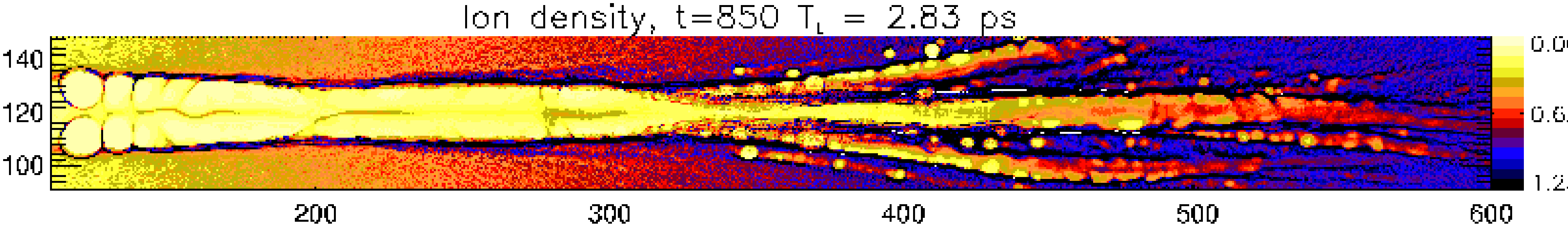

Pulse front: beam breakup
and EM **cavitons**

Left channel side:
 "hybrid" quasi-periodic structures,
"part **soliton**,
part **vortex**"...

Lyseikina et al,
arXiv:physics/0701139

Macchi et al,
PPCF **49** (2007) B71

Bigongiari et al,
in preparation

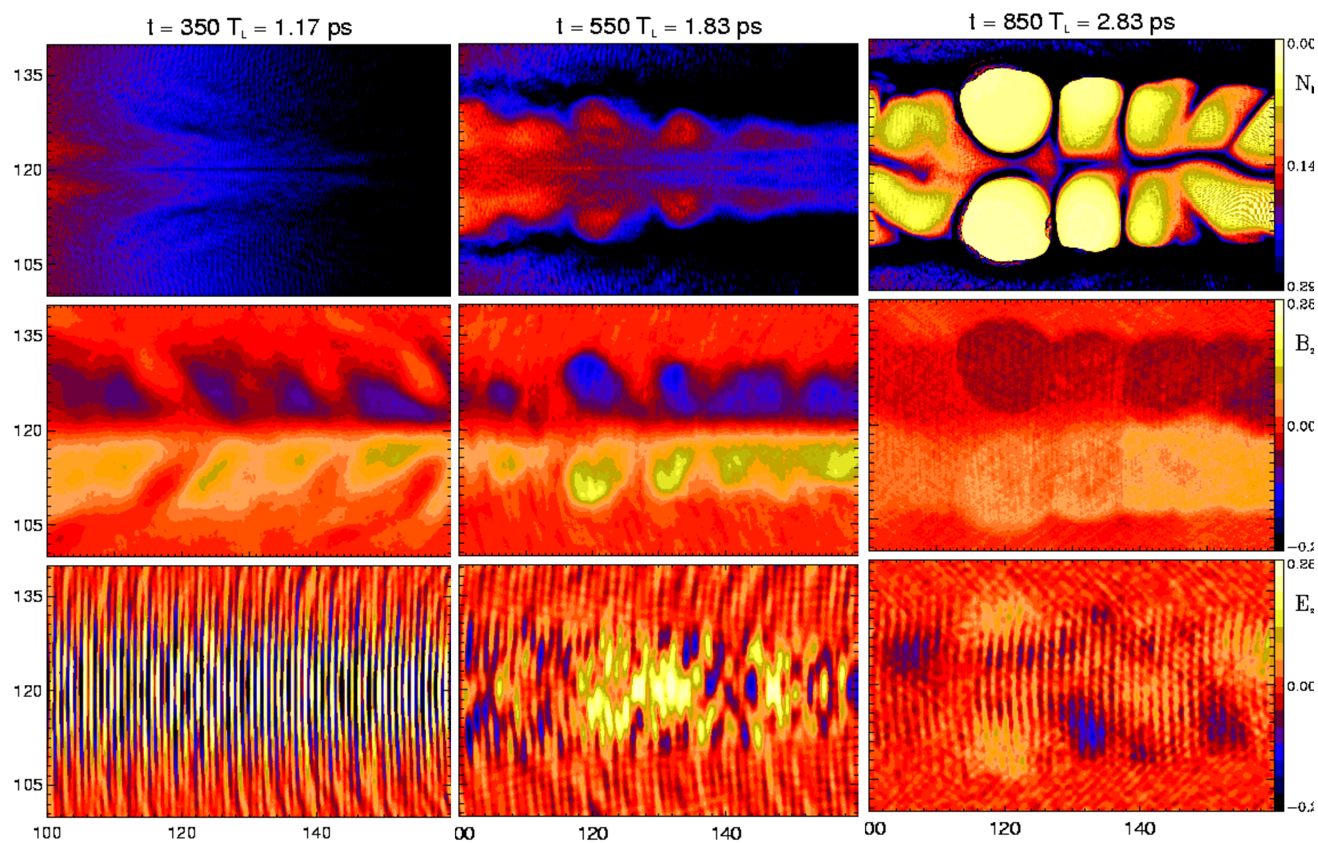

Simulation of proton images data: magnetic vortices?

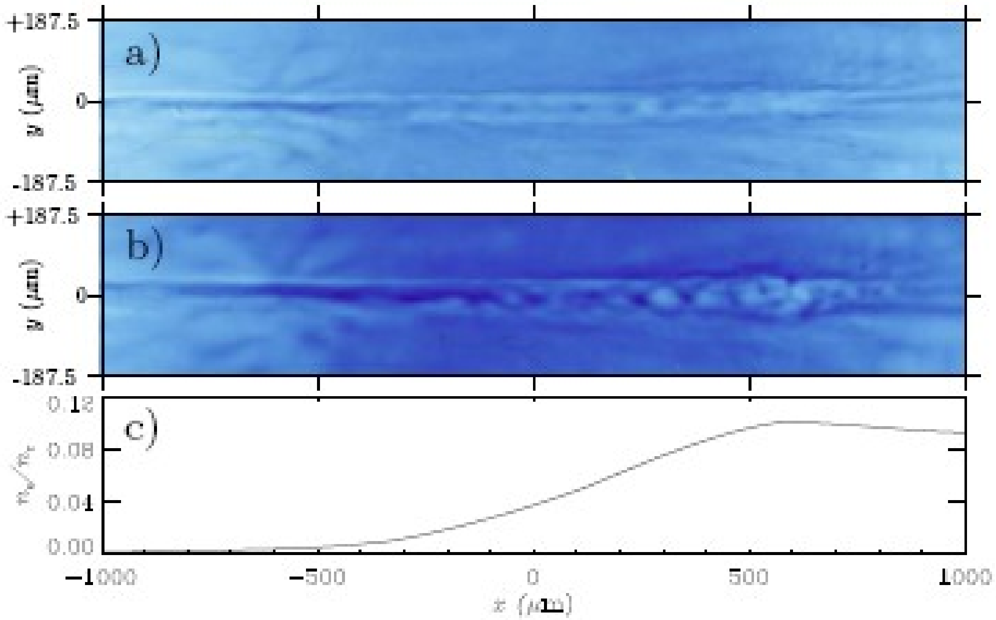

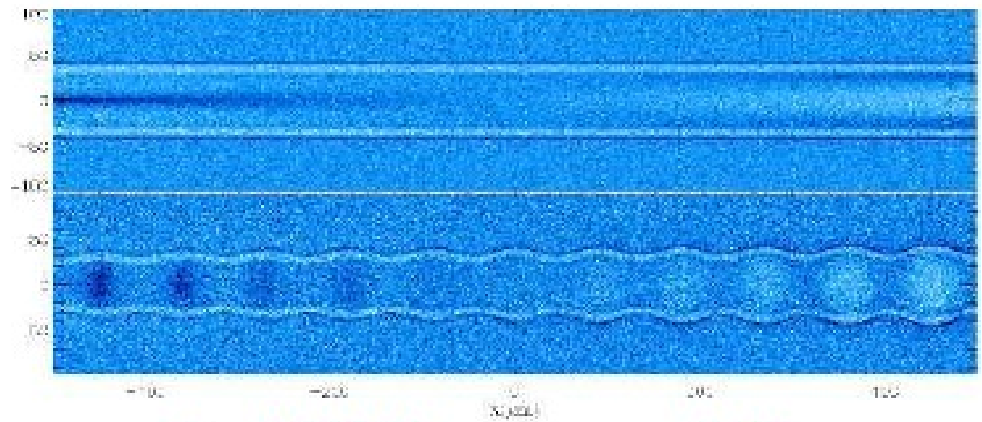

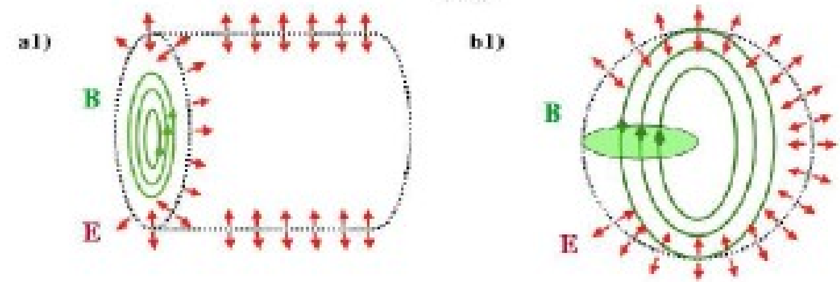

The 3D topology of the “coherent”, slowly evolving structures was inferred heuristically from 2D PIC simulations and used as an input for the particle tracing code producing synthetic proton images.

The comparison suggests that image formation is dominated by magnetic field deflections and suggests the formation of patterns of “magnetized vortex rings” along the channel

Bigongiari et al, in preparation

Several basic phenomena observed by proton probing

Bubble-like structures interpreted as remnants of **relativistic solitons** (“post-solitons”)
[Borghesi et al., Phys. Rev. Lett. **88** (2002) 135002]

Ion modulations resulting from onset and evolution of **Buneman instability** in the late evolution of a plasma wake
[Borghesi et al., Phys. Rev. Lett. **94** (2005) 195003]

Collisionless shock waves in the plasma blow-off
[Romagnani et al., Phys. Rev. Lett. **101** (2008) 025004]

Coherent **“Hybrid” magnetic structures** in a self-focusing channel
[Bigongiari et al., in preparation]

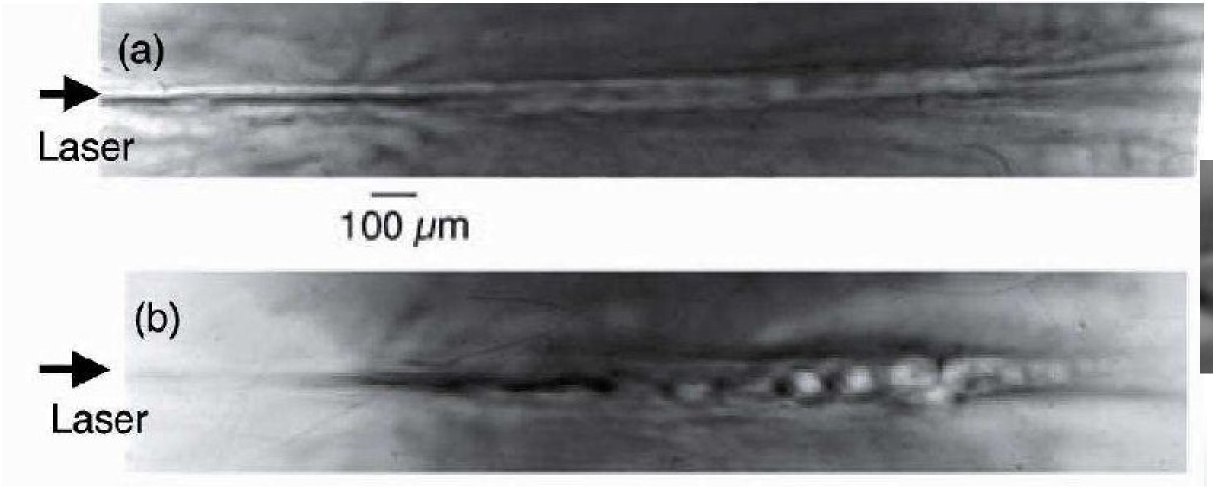

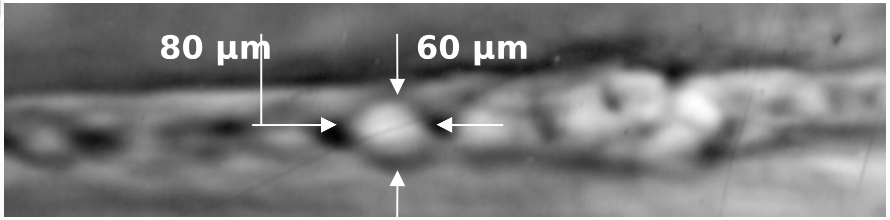

Dynamic control of proton beam properties

Concept: achieve **focusing** and **energy selection** of the proton beam by "external" devices or by "target engineering"

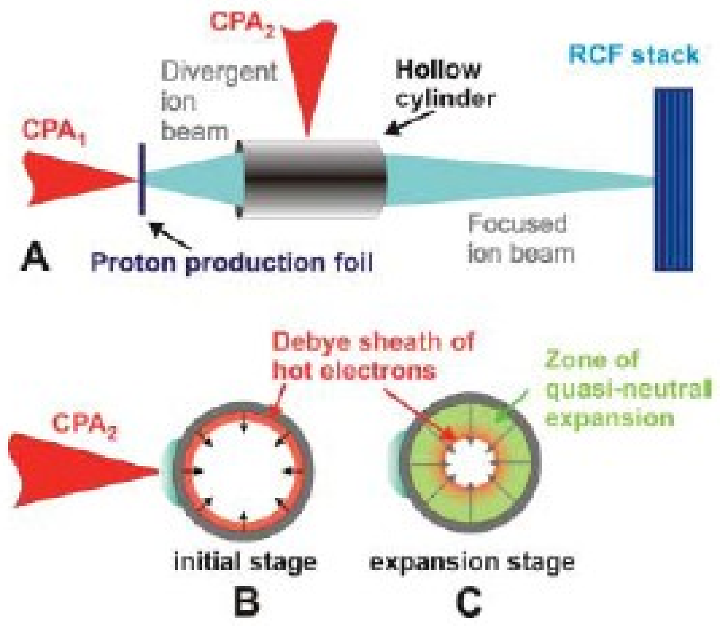

Laser-driven cylindrical microlens
Toncian et al., Science **312** (2006) 410

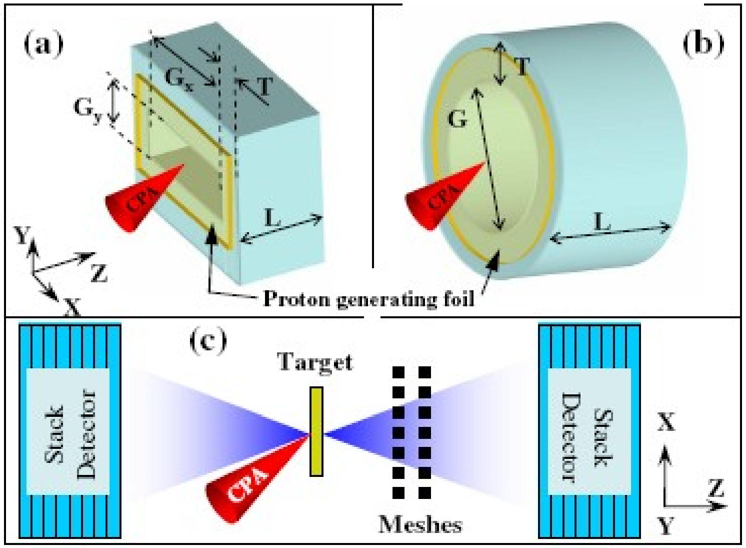

Shaped targets designed as **electrostatic (?) lenses**
Kar et al., PRL **100** (2008) 105004

Both approaches pose the question on **how rapidly** the electric field created by escaping electrons propagates on the surface of the target

Field propagation on the rear surface of solid targets

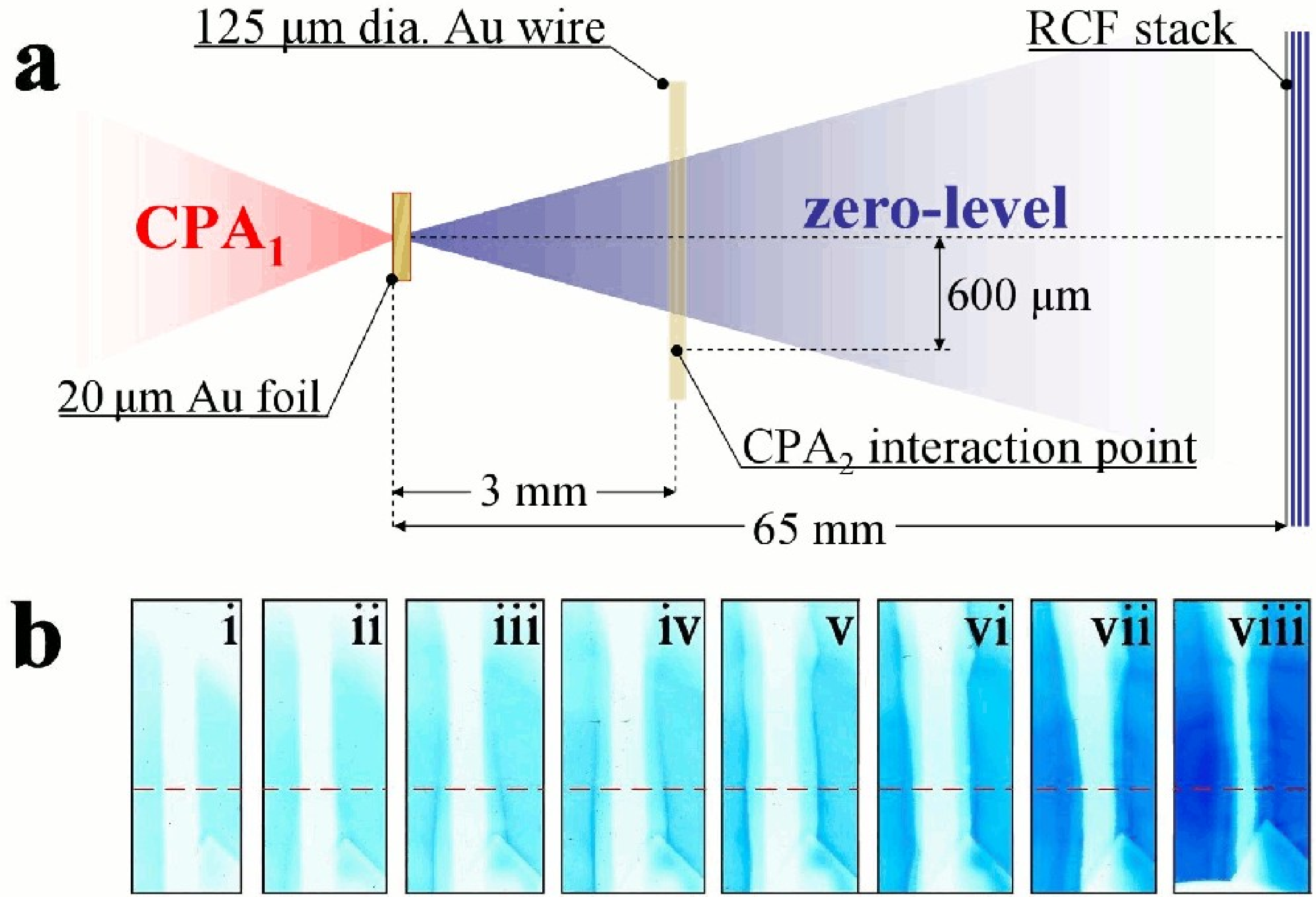

- In the interaction with a wire target a fast positive charging followed by later discharging is observed: escape of fast electrons and return neutralizing current?
- The propagation of the field out of the interaction region is not resolved with a "vertical" wire

K. E. Quinn et al, submitted to PRL

Field propagation on the rear surface of solid targets

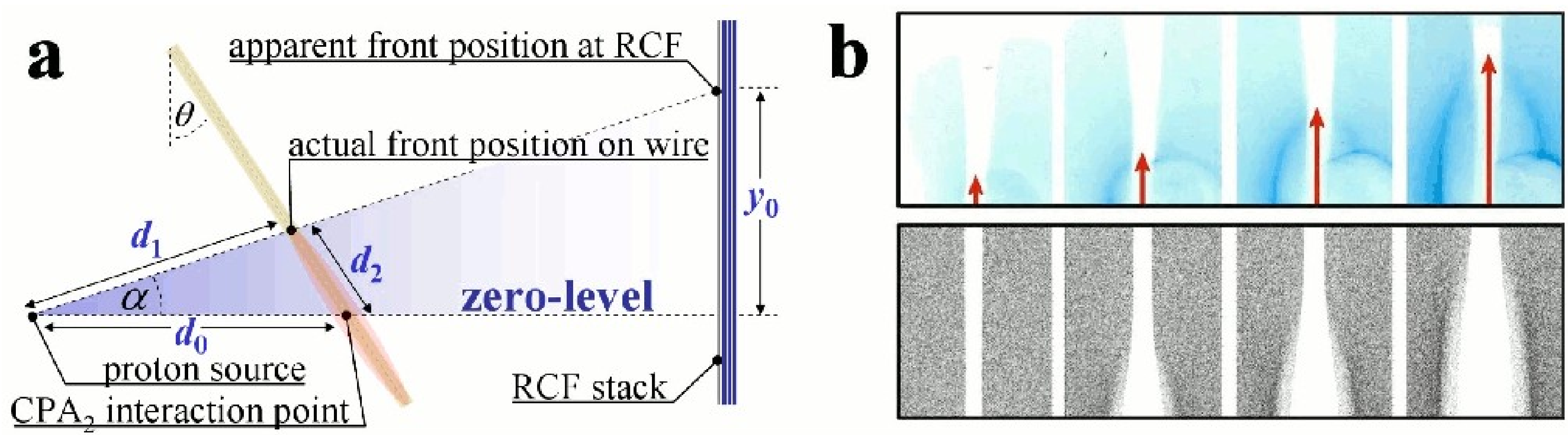

By inclining the wire to an angle θ with respect to the vertical axis the propagation of the field is resolved now ;

the speed v_f=0.96±0.04c

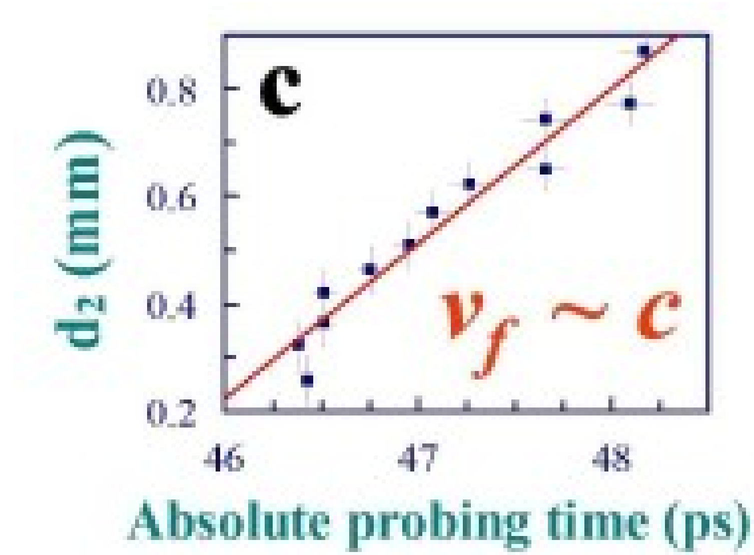

K. E. Quinn et al, submitted to PRL

Field propagation on the rear surface of solid targets

From the measurement of the radial field E_r and the propagation velocity v_f it is possible to reconstruct the history of the total current I flowing trough the wire

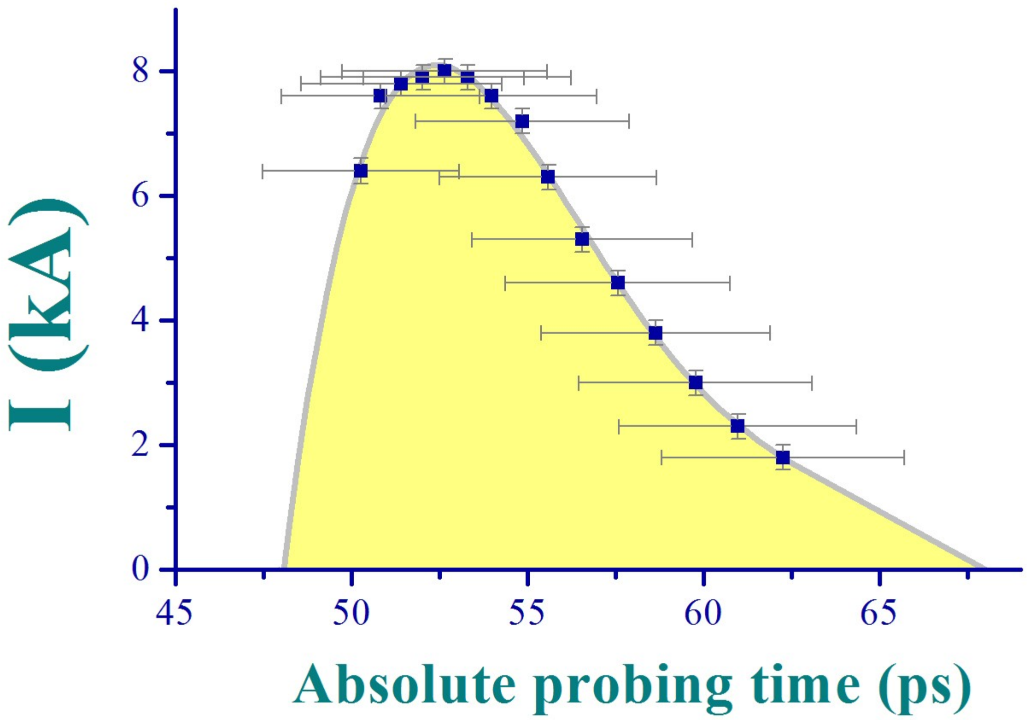

The estimate of the fraction of electrons escaped in vacuum f_{esc} thus obtained is roughly consistent with a simple estimate based on the charging of an “hot” plasma sphere or radius r_0 with N_e electrons in Boltzmann equilibrium

$$\frac{\ln f_{\mathrm{esc}}}{f_{\mathrm{esc}}} = -\frac{r_c}{r_0}\frac{m_e c^2}{k_B T_e} N_e$$

K. E. Quinn et al, submitted to PRL

Field propagation on the rear surface of solid targets

PIC simulations of a “model problem” show a “double front” structure of the current at the rear surface:

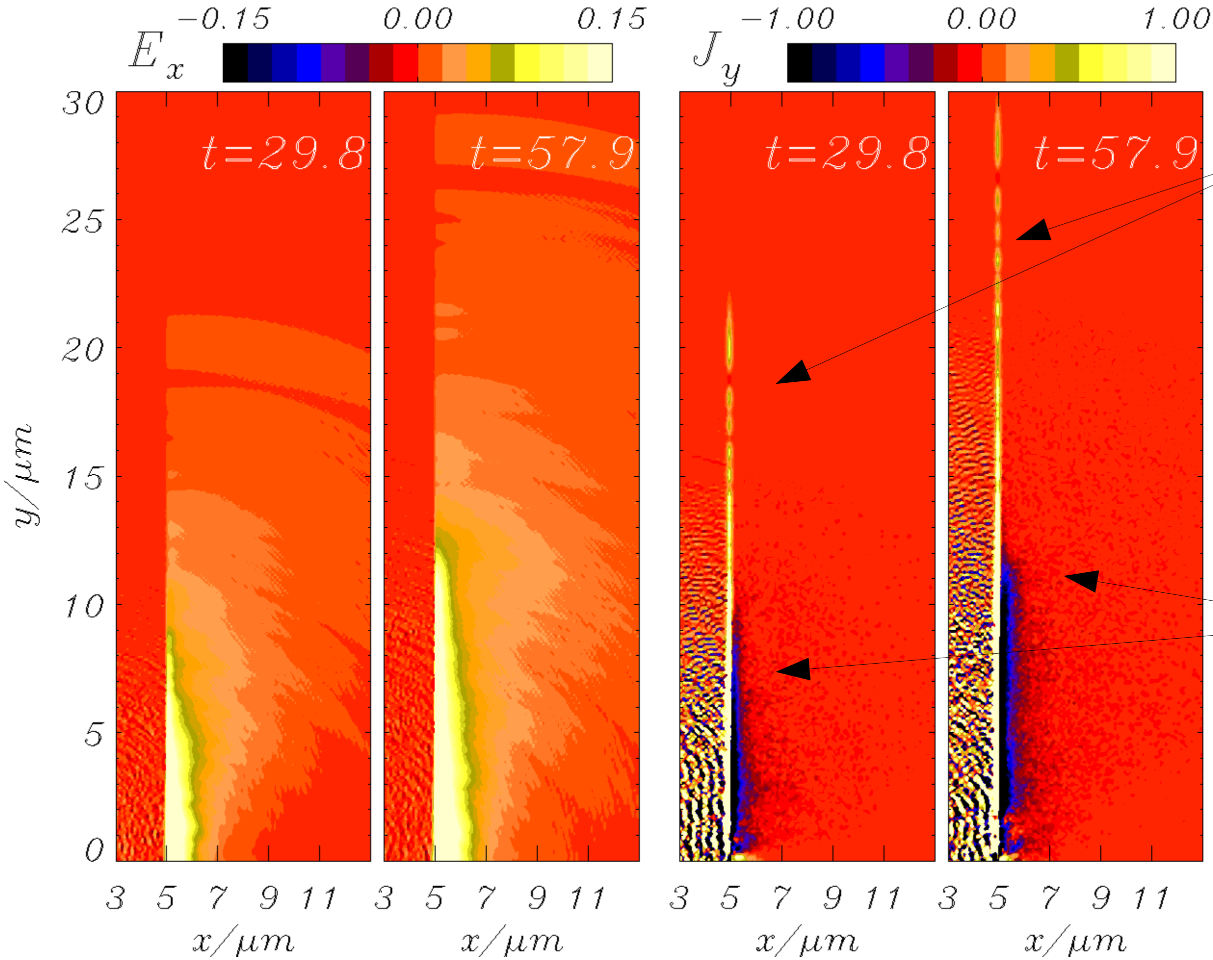

- thin current layer on the surface, propagating at speed c
-> driven by EM fields by the transient “antenna” created by escaping electrons

- bulk current of “fast” electrons, propagating slower than c
-> due to the spread of “fast” electrons in the transverse direction

K. E. Quinn et al, submitted to PRL

Field propagation on the rear surface of solid targets

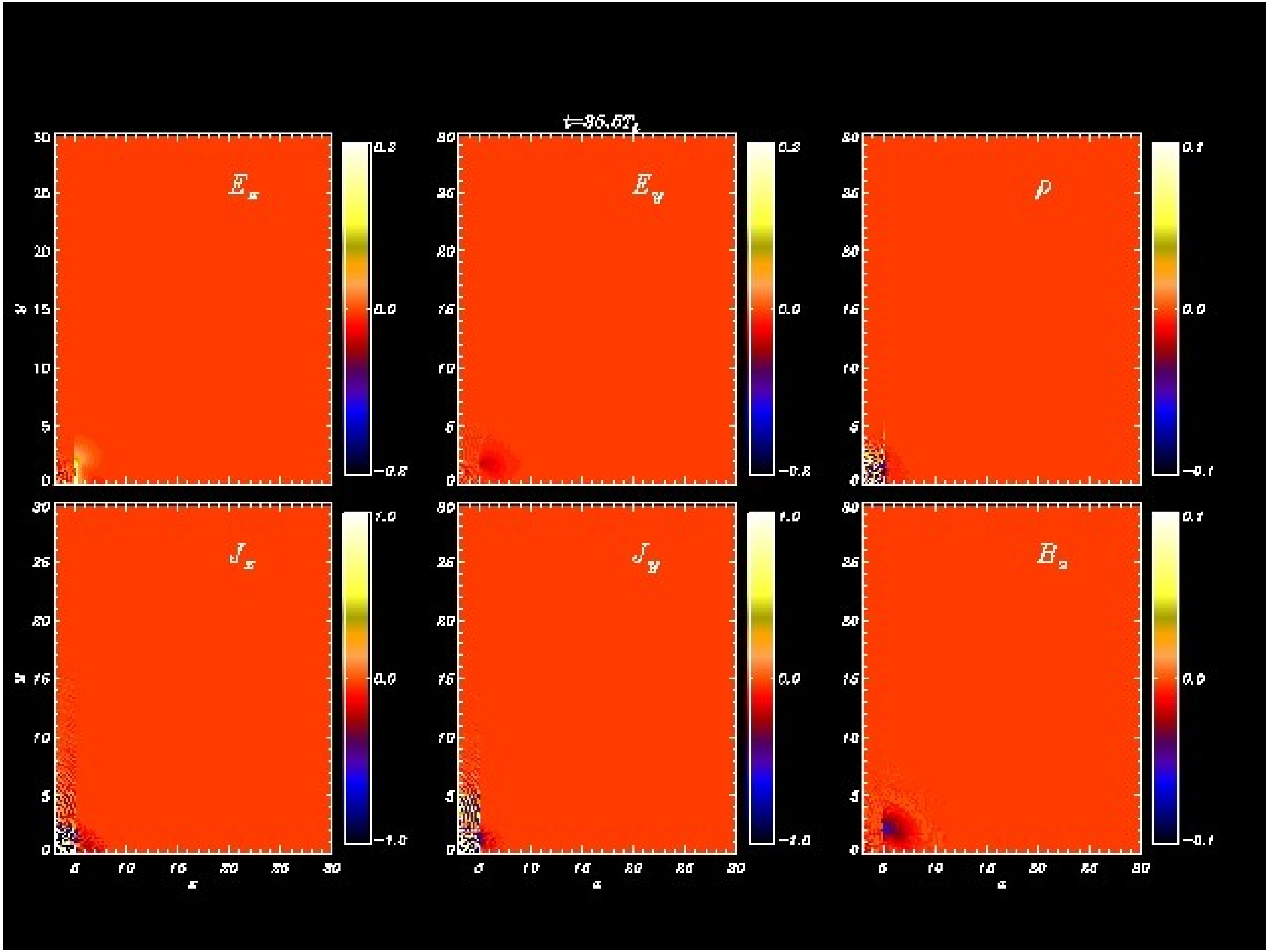

Field propagation on the rear surface of solid targets

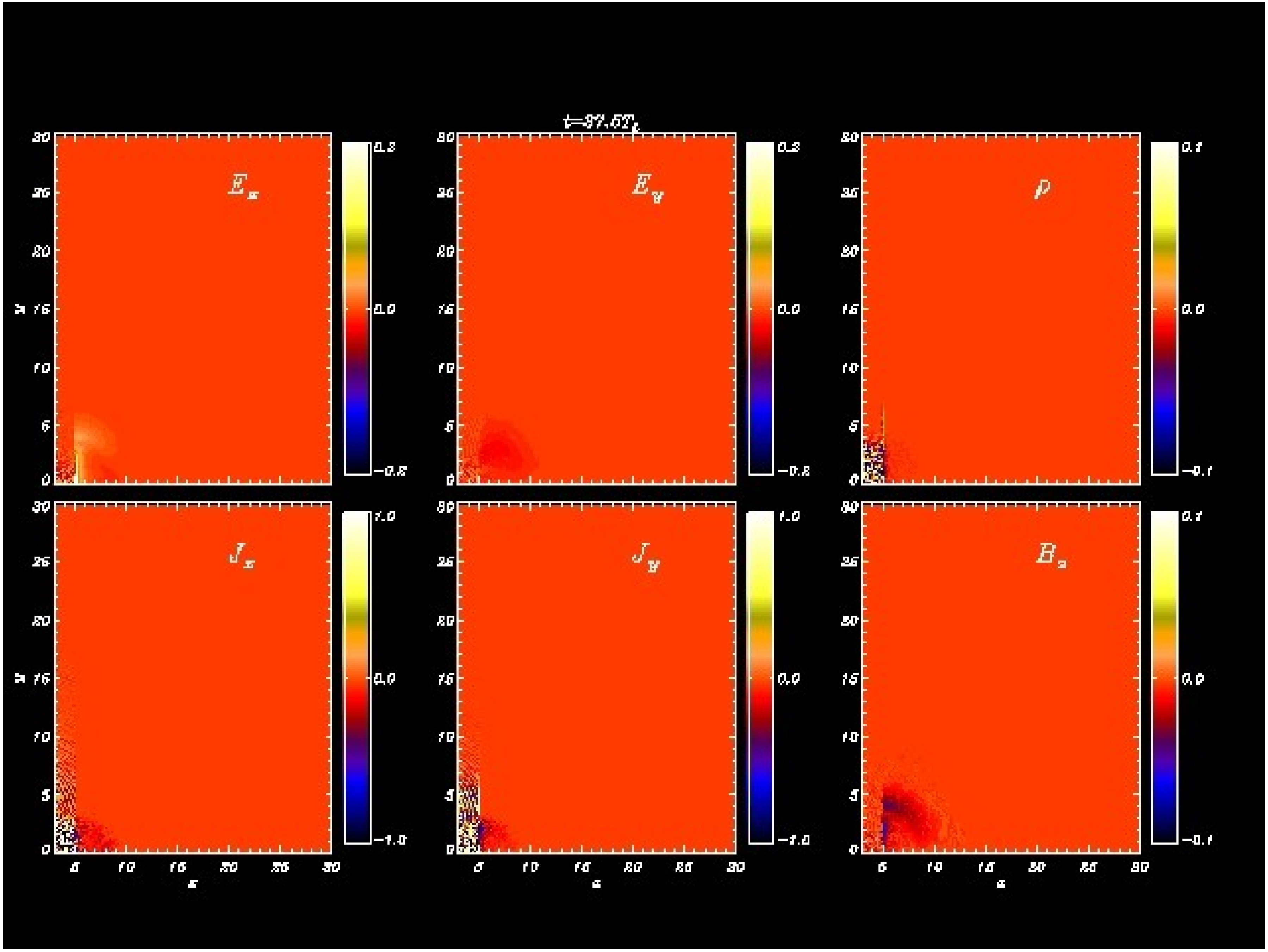

Field propagation on the rear surface of solid targets

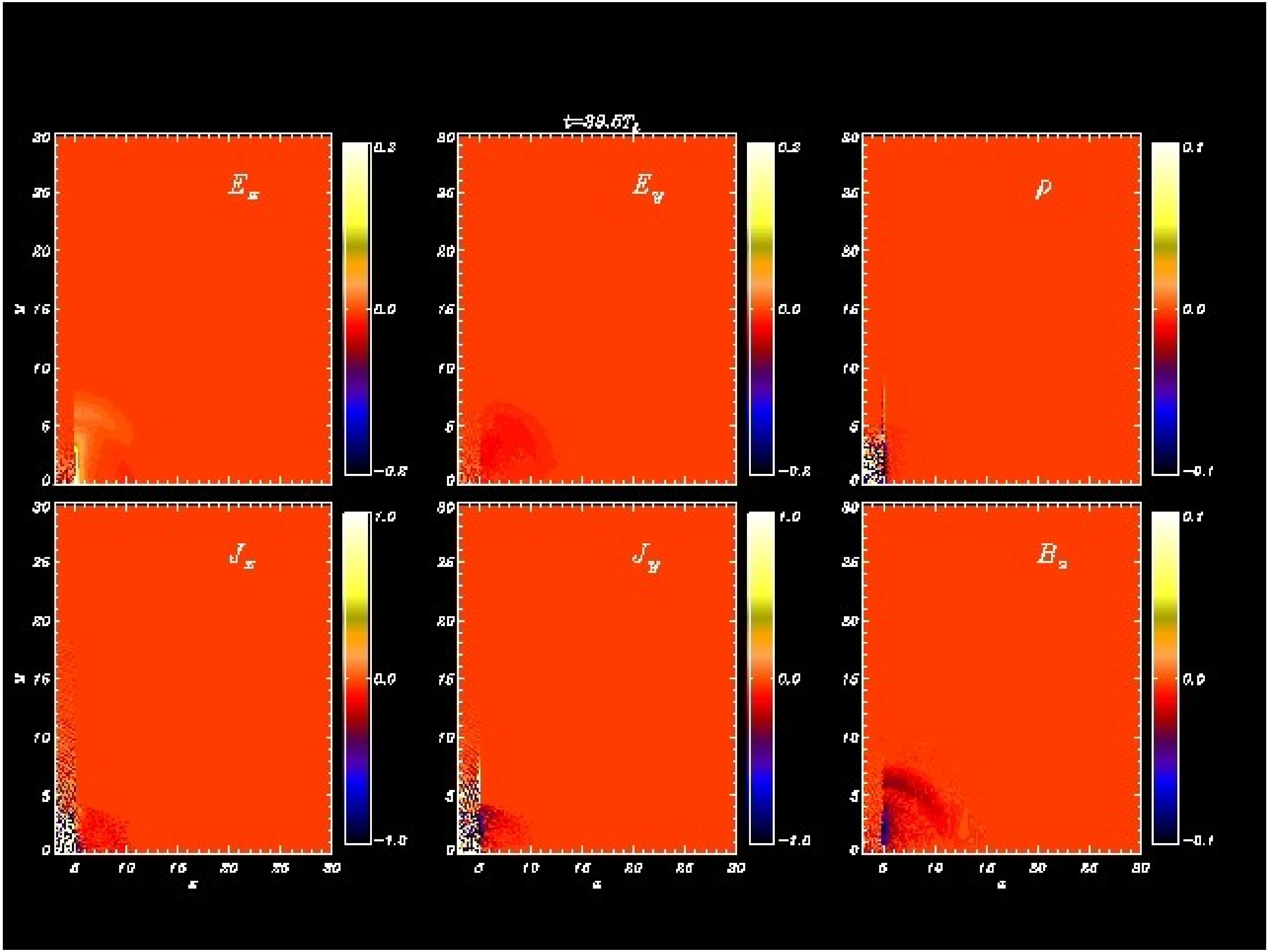

Field propagation on the rear surface of solid targets

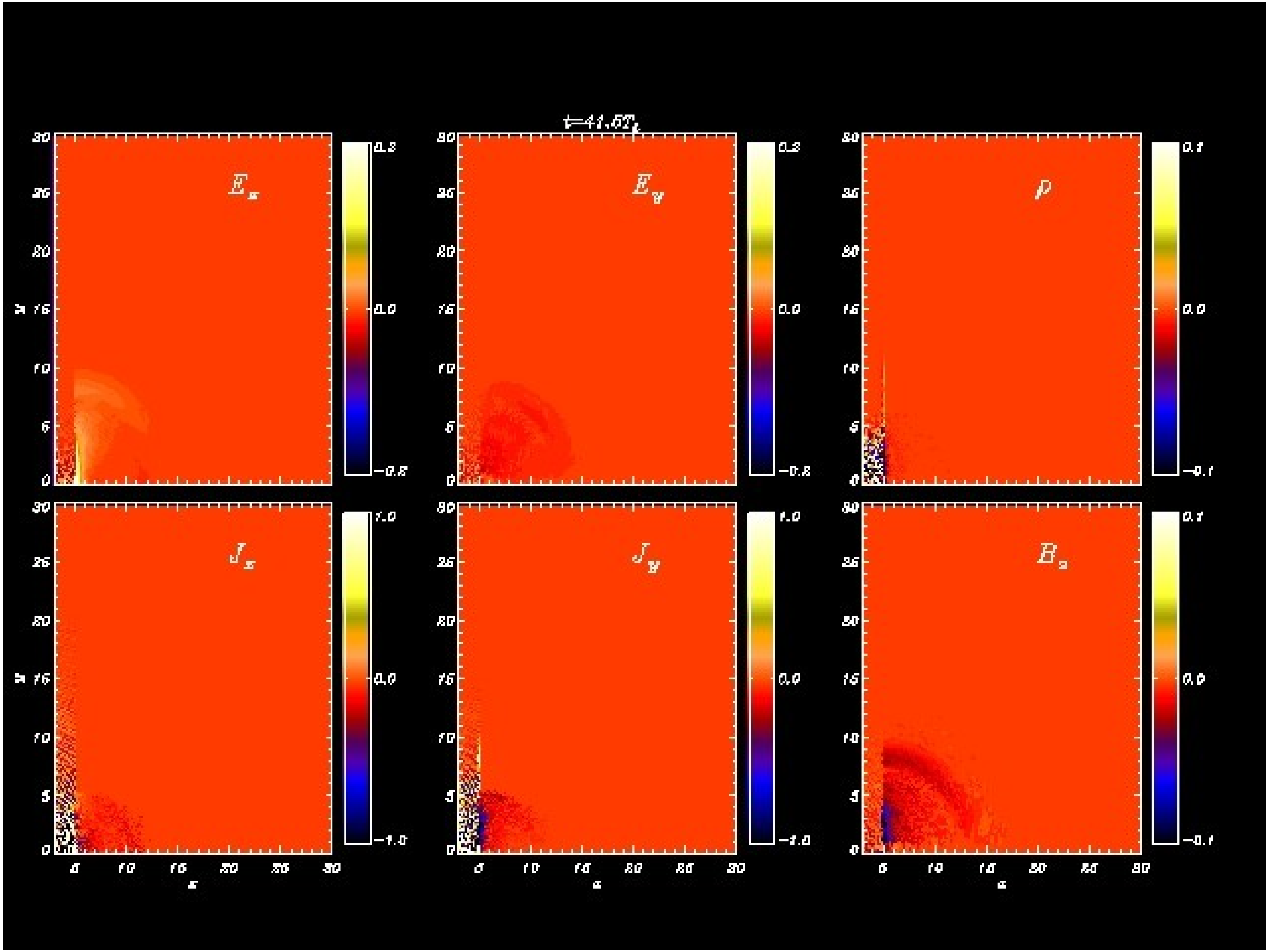

Field propagation on the rear surface of solid targets

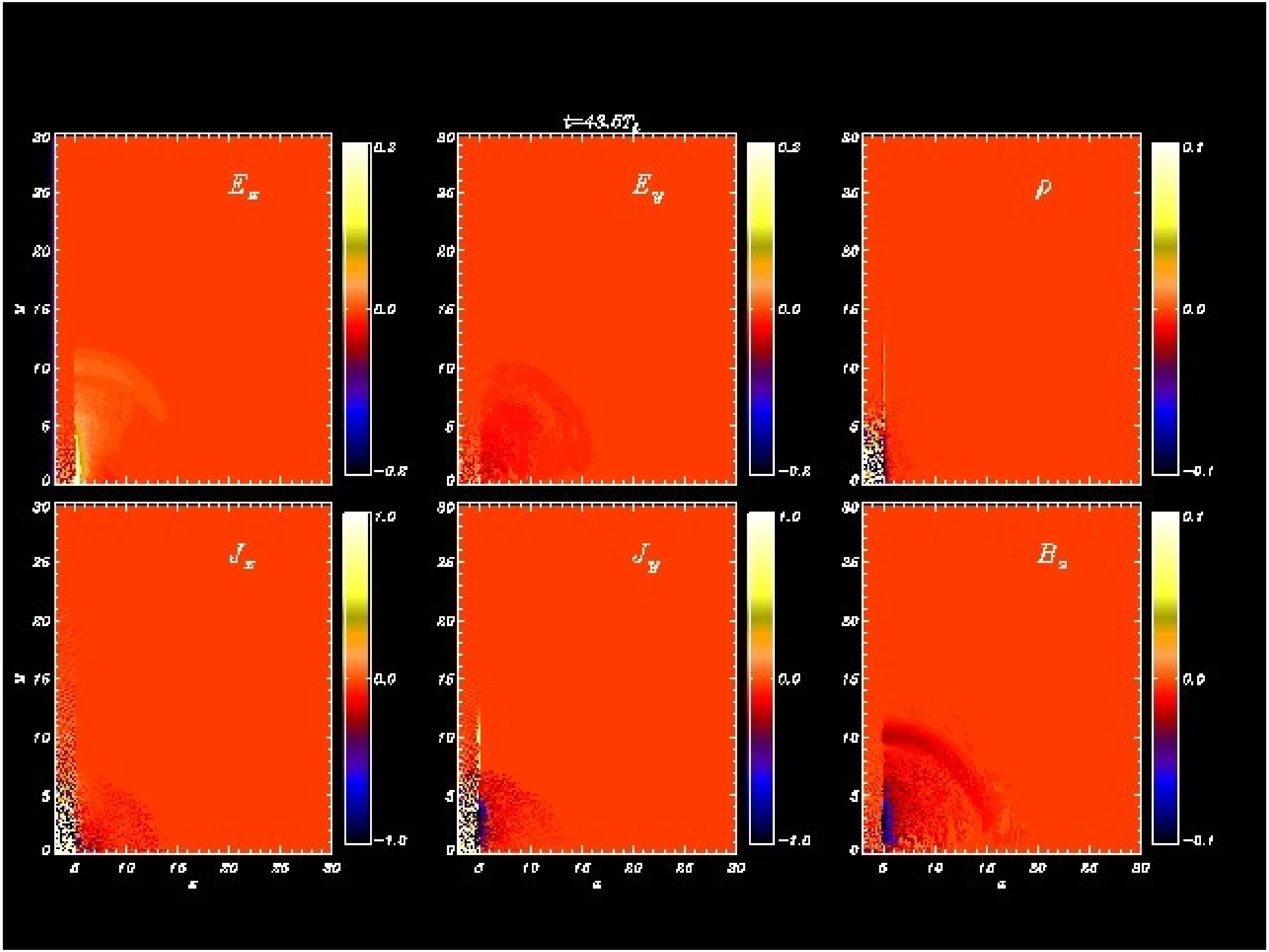

Field propagation on the rear surface of solid targets

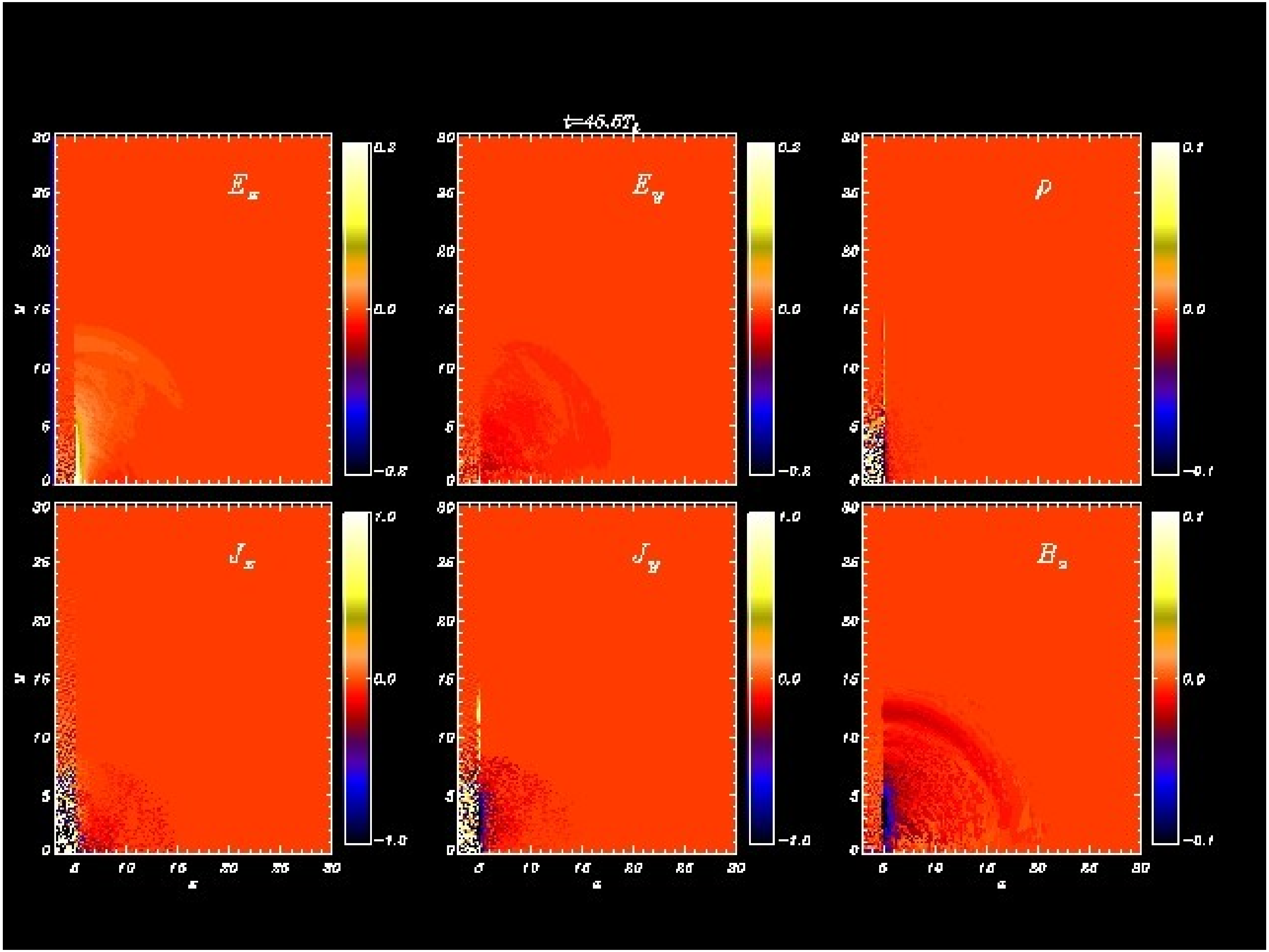

Field propagation on the rear surface of solid targets

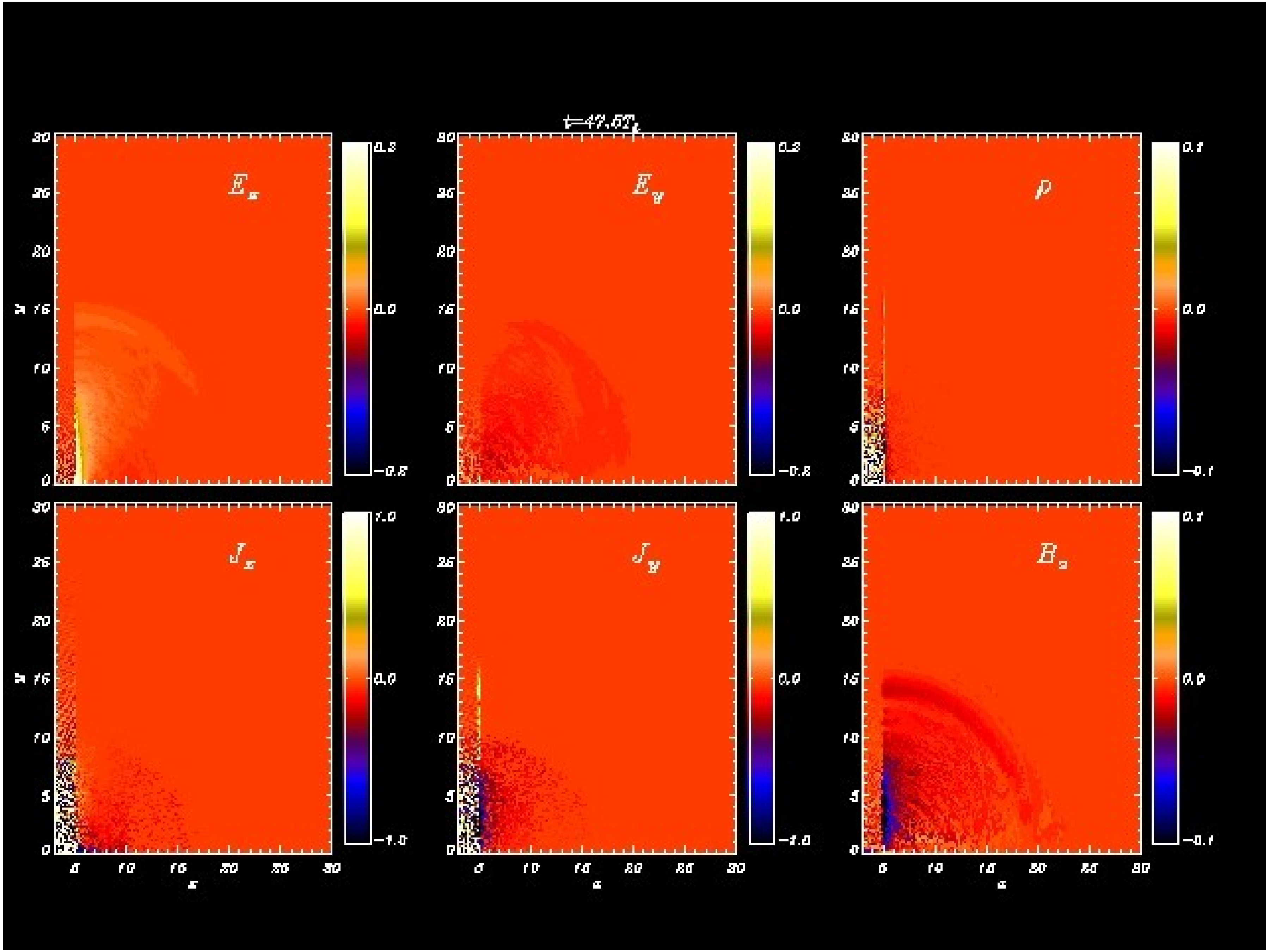

Field propagation on the rear surface of solid targets

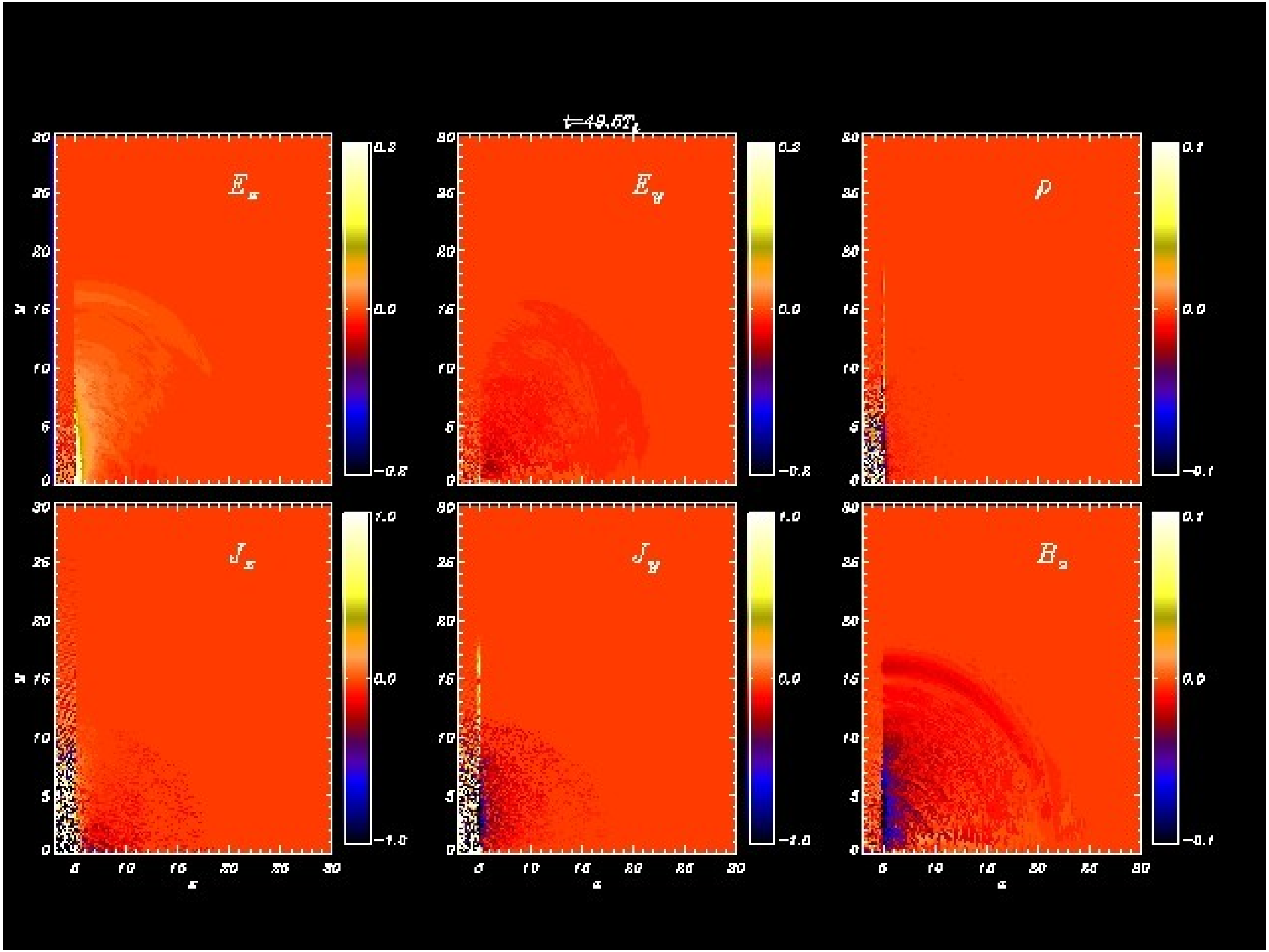

Field propagation on the rear surface of solid targets

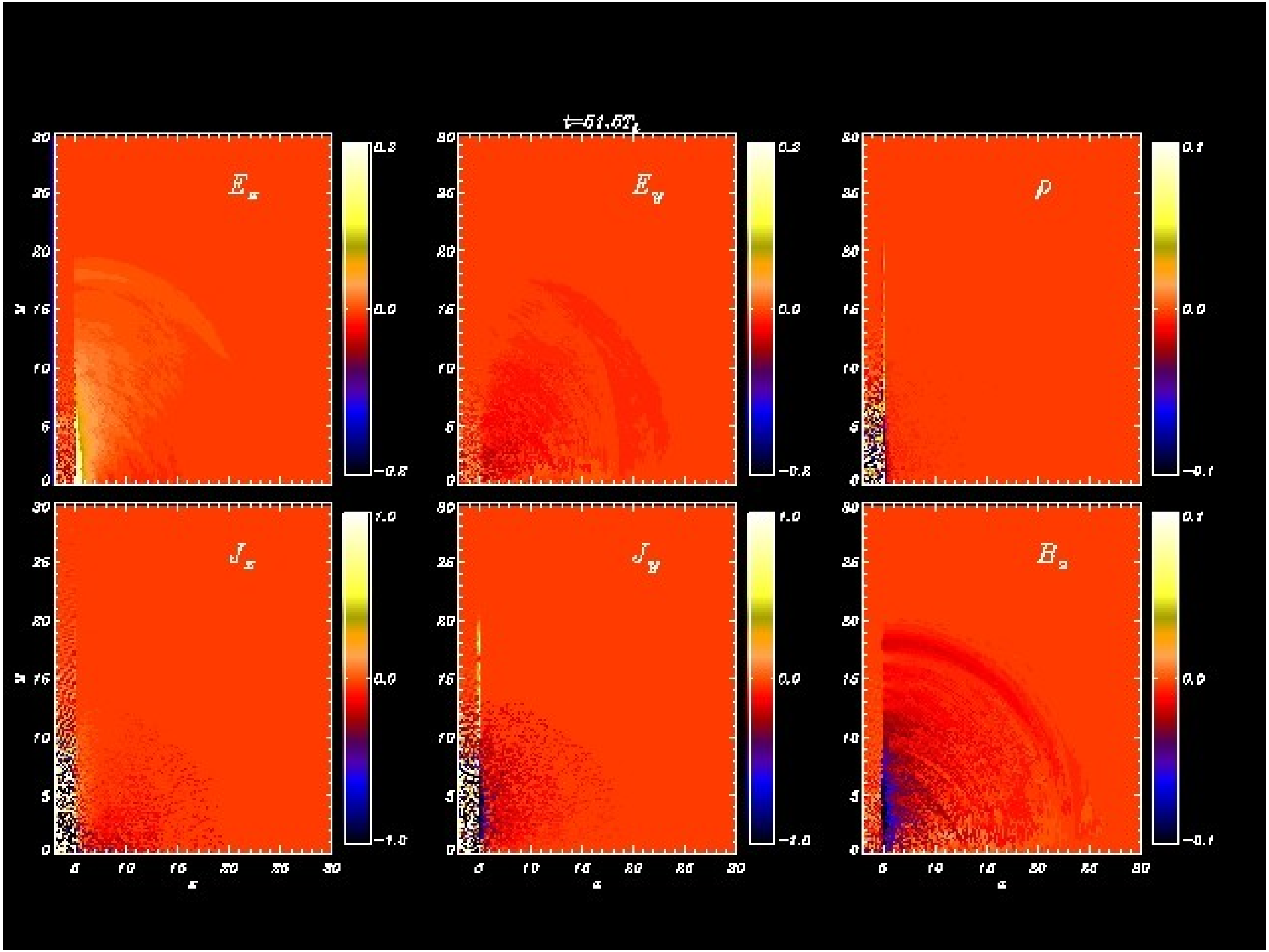

Field propagation on the rear surface of solid targets

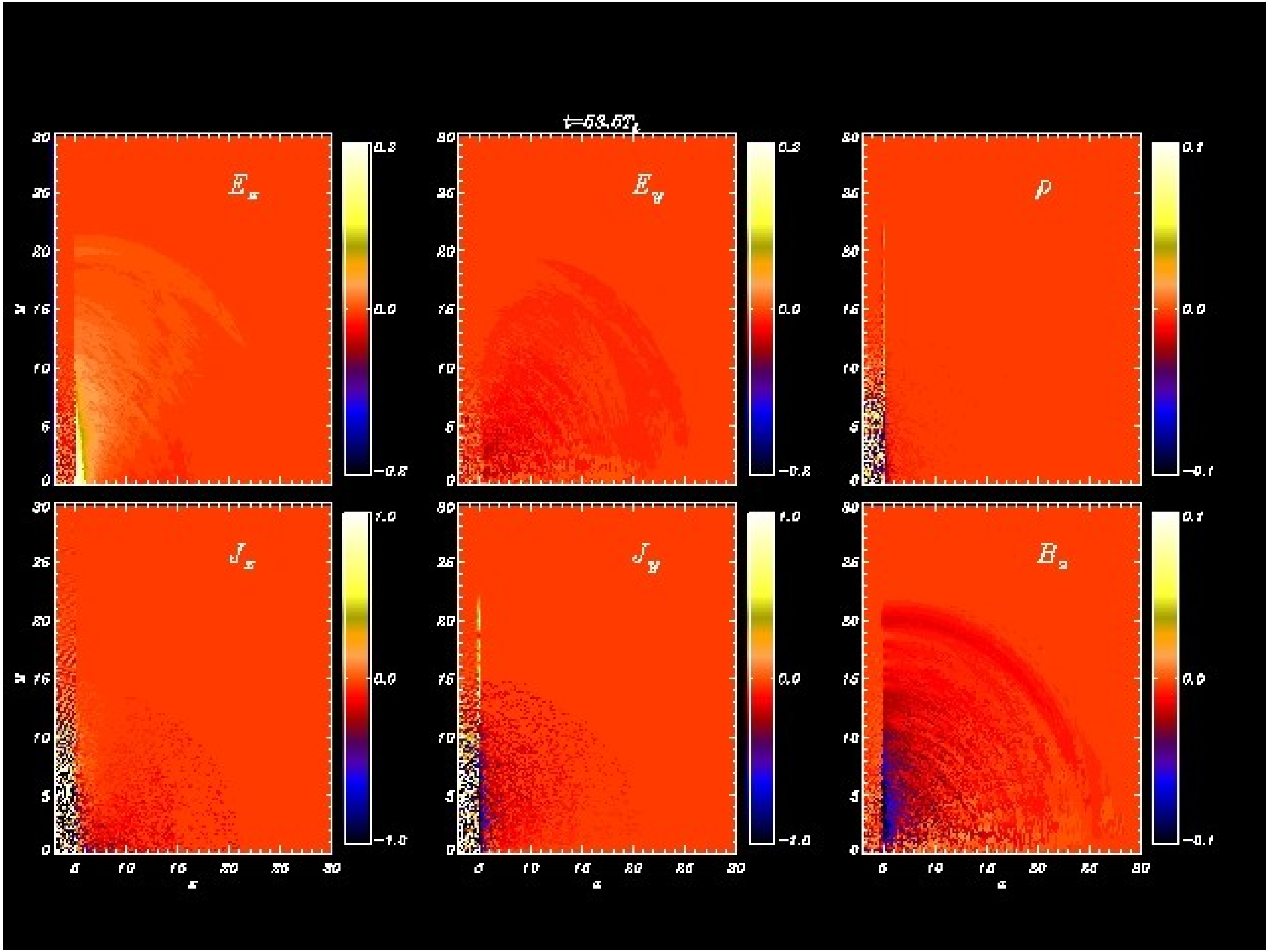

Field propagation on the rear surface of solid targets

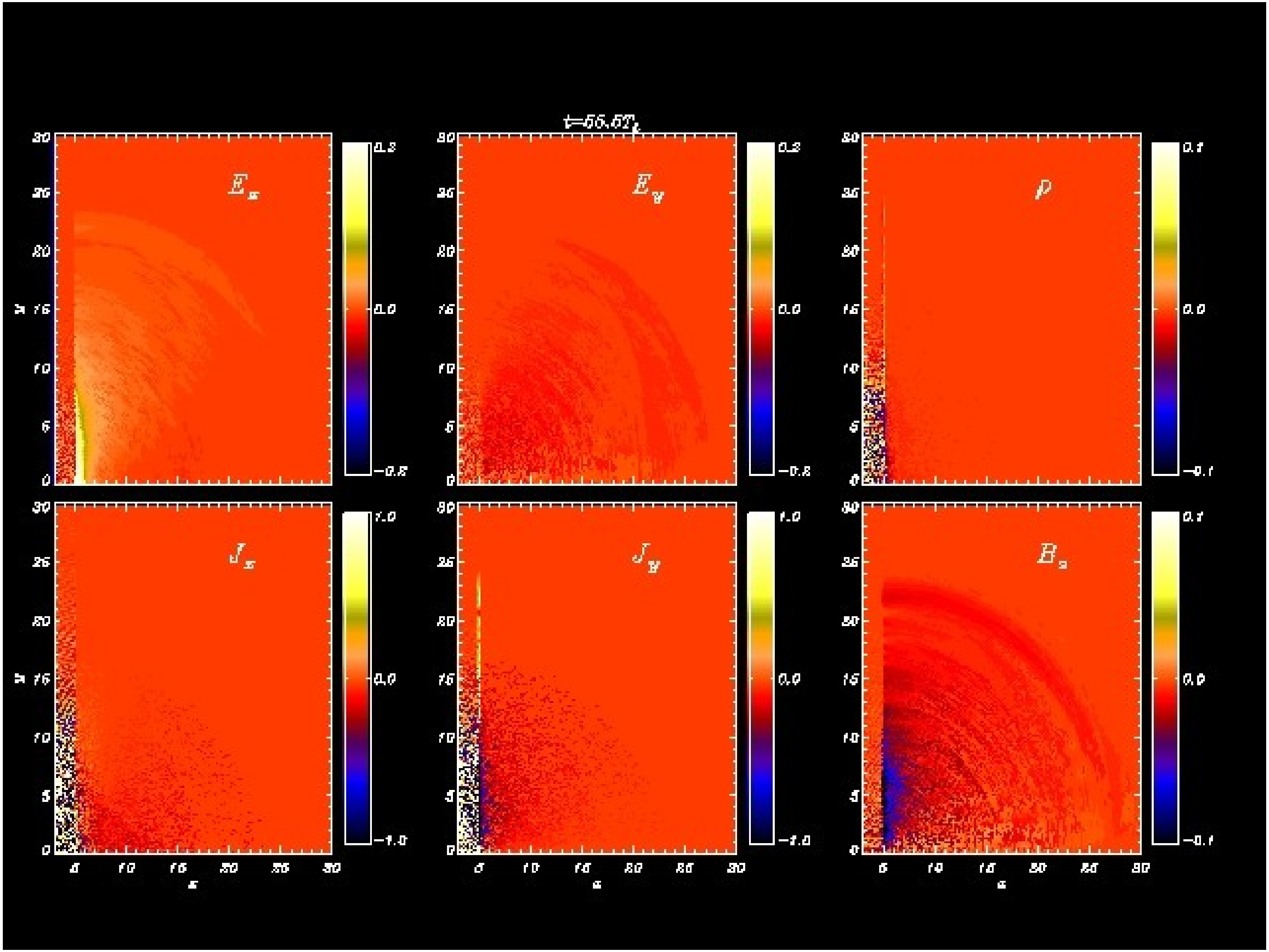

Field propagation on the rear surface of solid targets

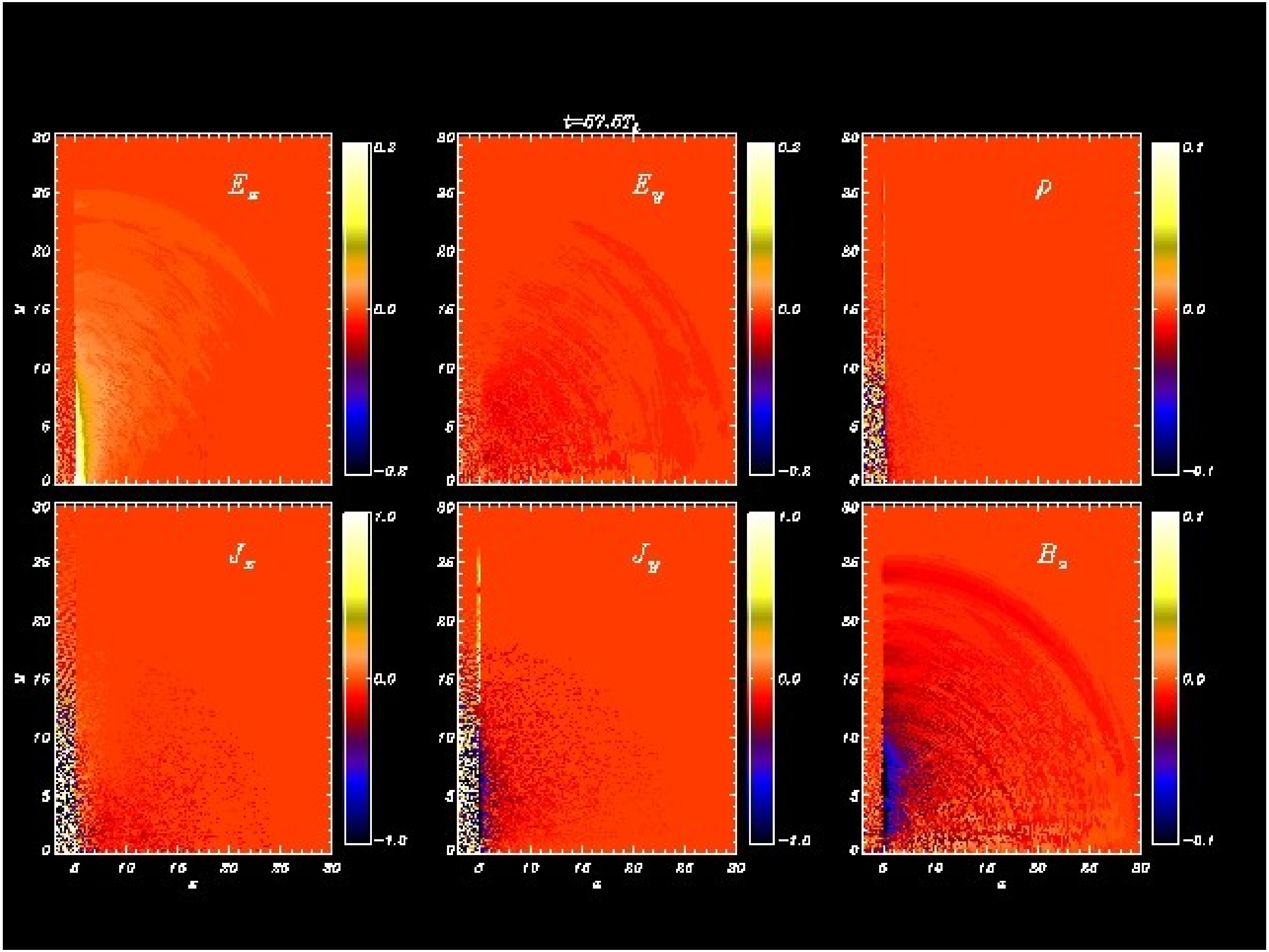

Field propagation on the rear surface of solid targets

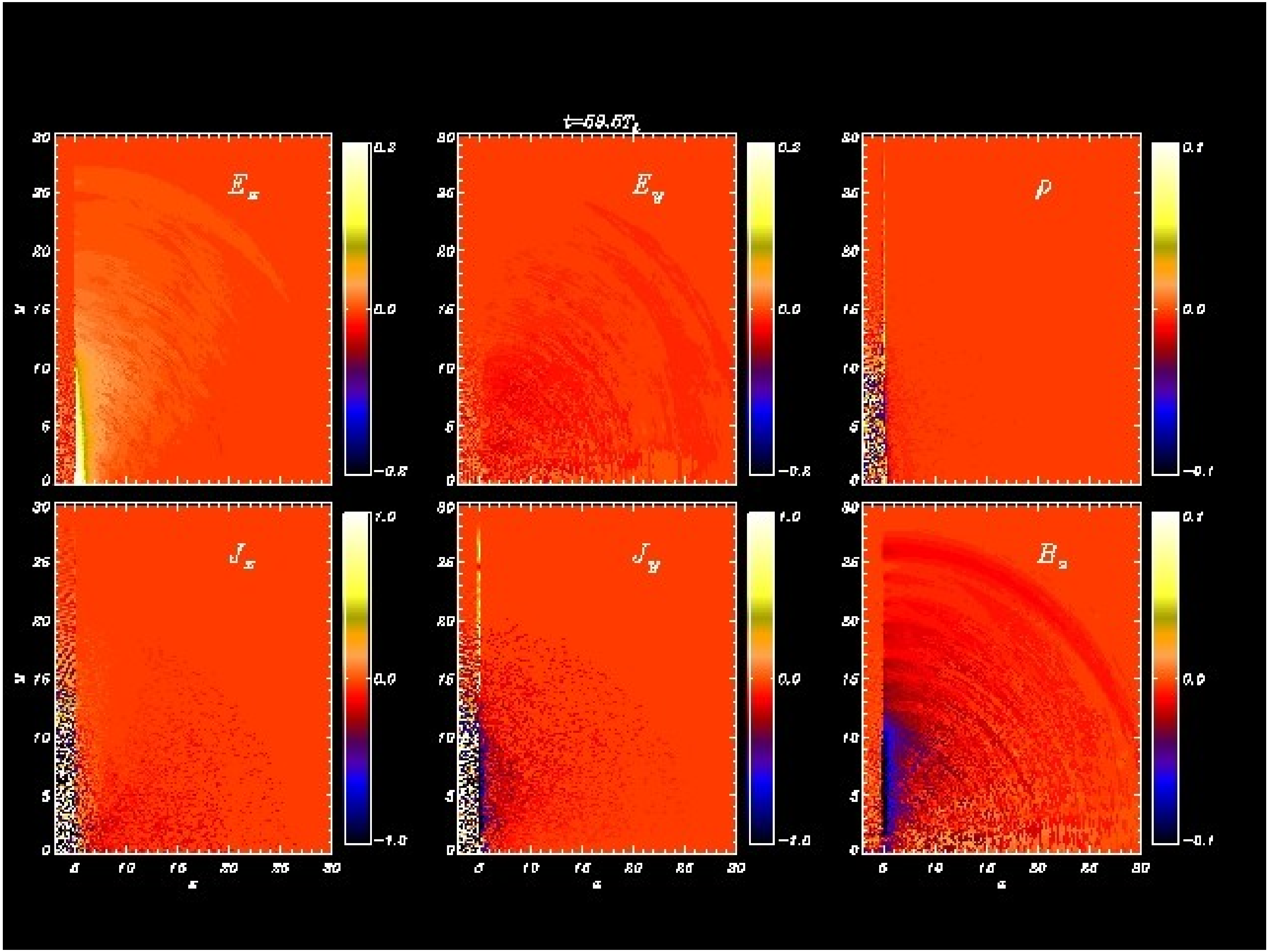

Field propagation on the rear surface of solid targets

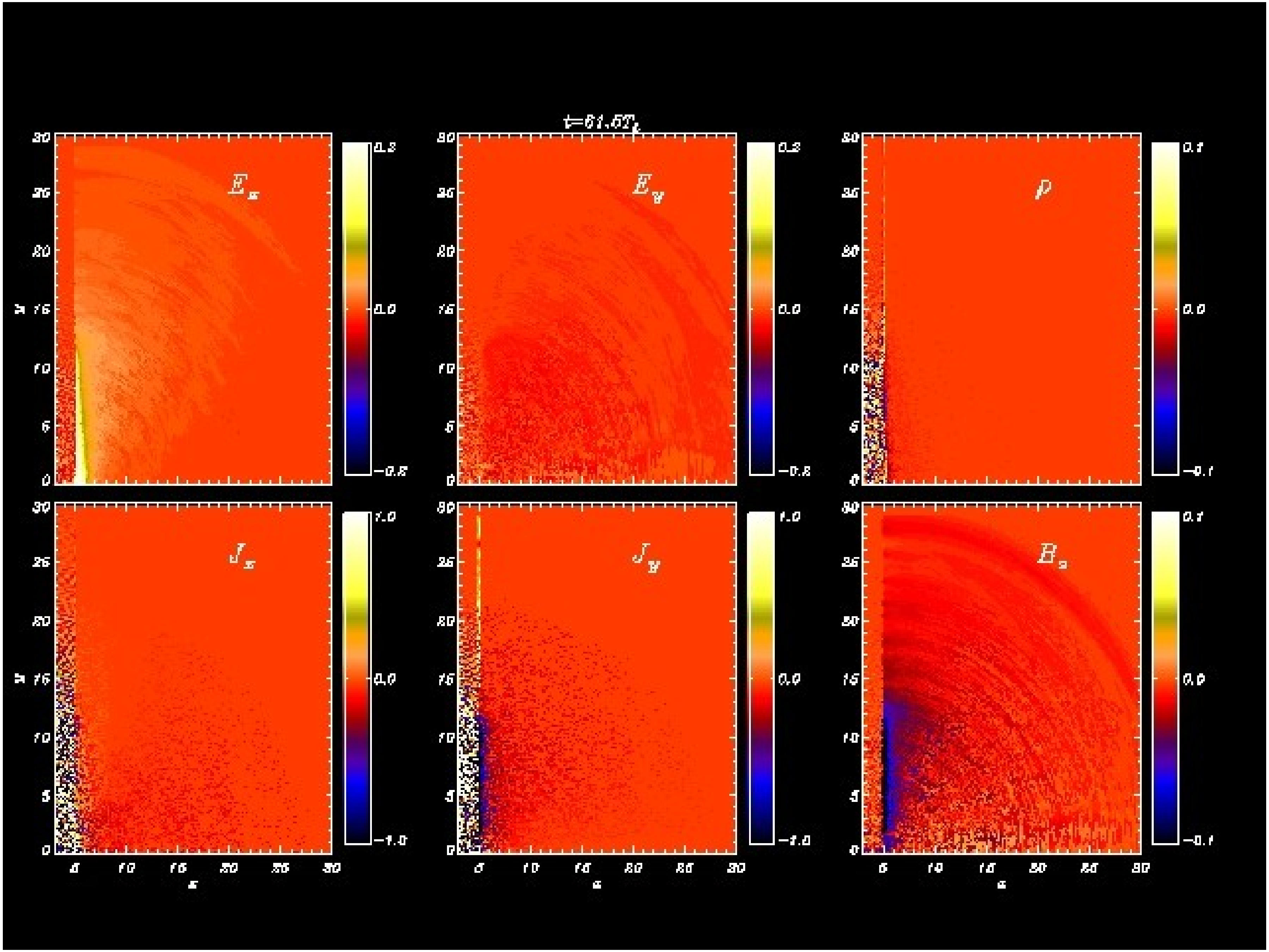

Some general considerations

• The proton probing technique allowed detailed space- and time-resolved measurement of EM fields in “laser plasmas” for the first time

• Several basic physical phenomena can be investigated

• However, results are qualitative or semi-quantitative because of:

  ➔ Weak control and characterization of plasmas

  ➔ Constraints on experimental set-up and geometry

  ➔ 3D imaging and EM simulations are both hard to perform

• Plasma physics theorists often hope for plasmas which can be more controlled and characterized ...

Ultracold Plasmas

Produced by (slightly above threshold) photoionization of a laser-cooled, magnetically trapped suitable gas

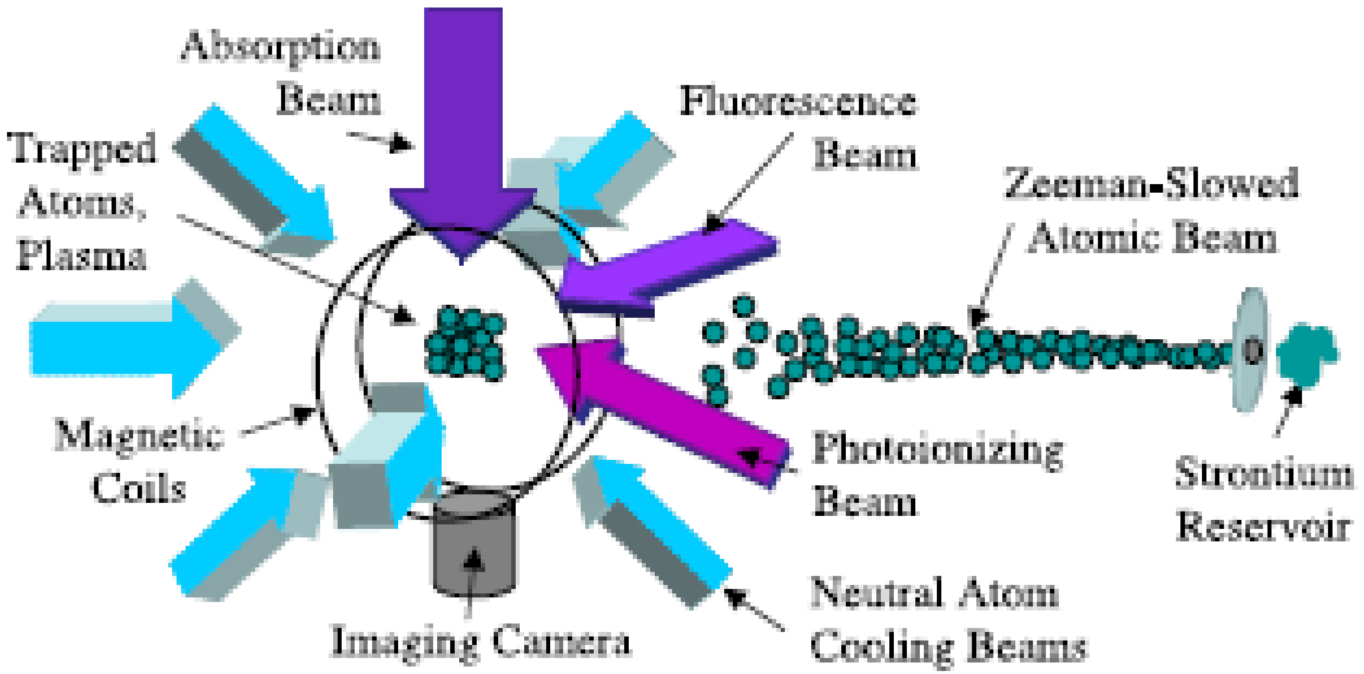

Figure 2. Experimental schematic for strontium plasma experiments. The MOT for neutral atoms consists of a pair of anti-Helmholtz magnetic coils and six laser-cooling beams. Atoms from a Zeeman-slowed atomic beam enter the MOT region and are trapped. $^1P_1$ atoms are ionized by the photoionizing laser. The absorption imaging beam passes through the plasma and falls on a CCD camera. The fluorescence beam propagation direction is perpendicular to the imaging axis.

T.C.Killian et al, Phys.Rev.Lett **83** (1999) 4776
T.C.Killian, Science **316** (2007) 705
T.C.Killian, T.Pattard, T.Pohl, J.M.Rost, Phys.Rep. **449** (2007) 77
J.Castro, H.Gao and T.C.Killian, Plasma Phys. Contr. Fus. **50** (2008) 124011

Ultracold Plasmas

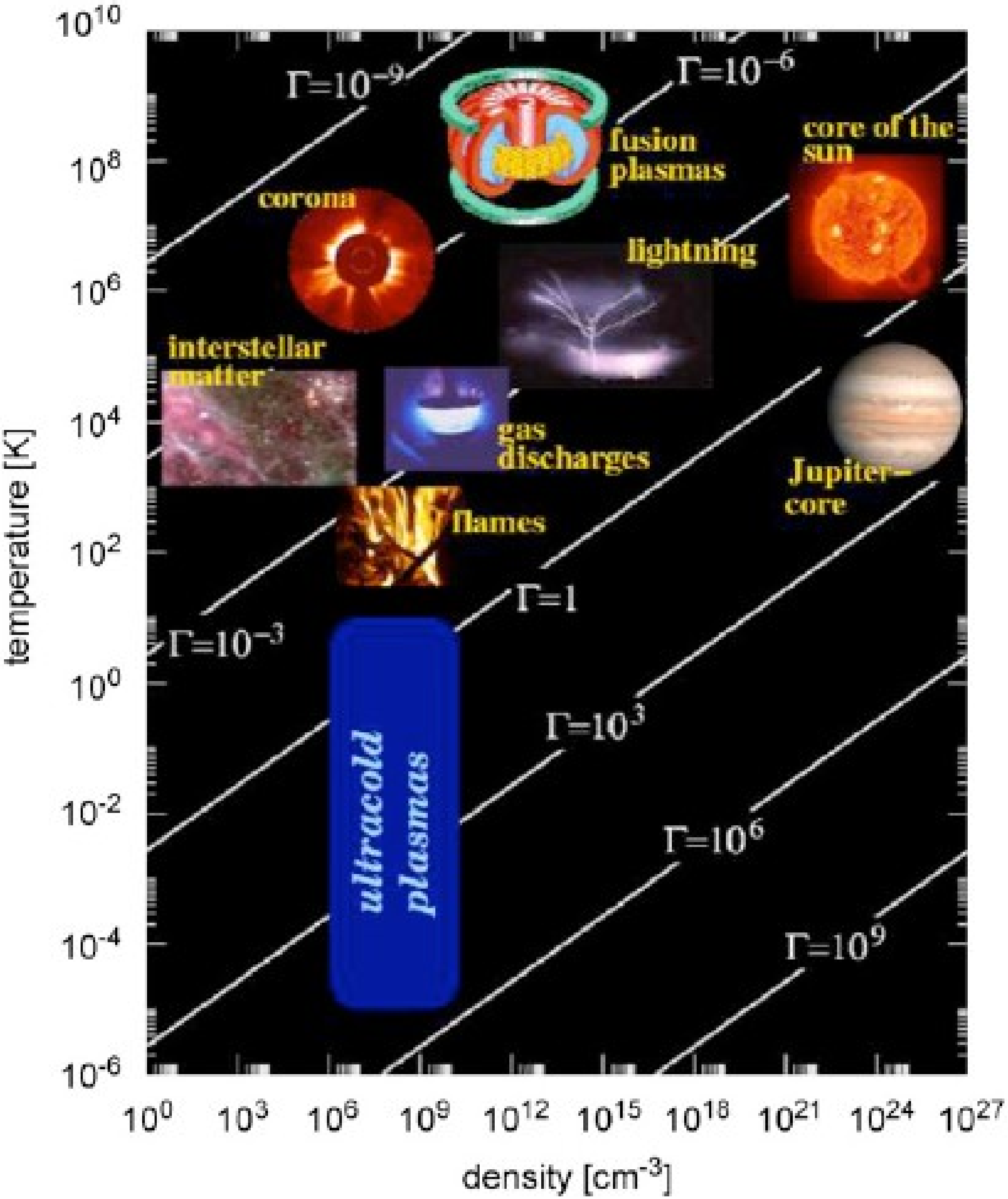

- density controlled by the number of atoms in the trap

- temperature controlled by the frequency of the photoionizing ionizing laser

- the plasma is most of the times in the strongly coupled regime

$\Gamma>1$

$$\Gamma = \frac{e^2/a}{k_B T}, \qquad a = \left(\frac{3}{4\pi n_i}\right)^{1/3}$$

Expansion of an Ultracold Plasma

PRL 99, 155001 (2007) PHYSICAL REVIEW LETTERS week ending 12 OCTOBER 2007

Experimental Realization of an Exact Solution to the Vlasov Equations for an Expanding Plasma

S. Laha,[1] P. Gupta,[1] C. E. Simien,[1] H. Gao,[1] J. Castro,[1] T. Pohl,[2] and T. C. Killian[1]
[1]*Department of Physics and Astronomy, Rice University, Houston, Texas 77005, USA*
[2]*ITAMP, Harvard-Smithsonian Center for Astrophysics, 60 Garden Street, Cambridge, Massachusetts 02138, USA*
(Received 14 May 2007; published 8 October 2007)

self-similar solution for a neutral plasma (*)

$$\left(\partial_t + \mathbf{v}\cdot\boldsymbol{\nabla} - \frac{q_\alpha}{m_\alpha}\mathbf{E}\cdot\partial_{\mathbf{v}}\right) f_\alpha(\mathbf{r},\mathbf{v},t) = 0, \qquad (\alpha = e, i)$$

$$n_\alpha = \int f_\alpha(\mathbf{r},\mathbf{v},t)d^3\mathbf{v}, \qquad n_e \simeq n_i$$

$$f_\alpha \propto \exp\left[-\frac{r^2}{2\sigma^2} - \frac{m_\alpha(\mathbf{v}-\mathbf{u})^2}{2k_BT_\alpha}\right],$$

$$\sigma = \sigma(t) = \sigma(0)(1+t^2/\tau^2)^{1/2}, \qquad T_\alpha = T_\alpha(t) = T_\alpha(0)(1+t^2/\tau^2)^{-1},$$

$$\mathbf{u} = \mathbf{u}(\mathbf{r},t) = \gamma(t)\mathbf{r}, \qquad \dot{\gamma} = \frac{k_B(T_e+T_i)}{m_i\sigma^2}$$

A.V.Baitin, K.M.Kuzanyan, J.Plasma Phys. **59** (1998) 83
D.S.Dorozhkina, V.E.Semenov, PRL **81** (1998) 2691

Expansion of an Ultracold Plasma

PRL 99, 155001 (2007) PHYSICAL REVIEW LETTERS week ending 12 OCTOBER 2007

Experimental Realization of an Exact Solution to the Vlasov Equations for an Expanding Plasma

S. Laha,[1] P. Gupta,[1] C. E. Simien,[1] H. Gao,[1] J. Castro,[1] T. Pohl,[2] and T. C. Killian[1]
[1]Department of Physics and Astronomy, Rice University, Houston, Texas 77005, USA
[2]ITAMP, Harvard-Smithsonian Center for Astrophysics, 60 Garden Street, Cambridge, Massachusetts 02138, USA
(Received 14 May 2007; published 8 October 2007)

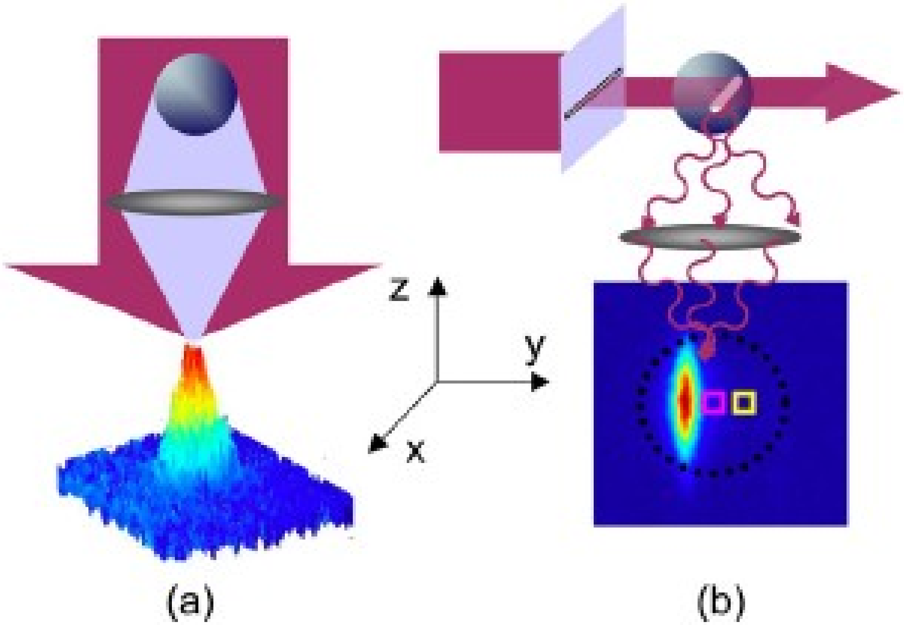

Figure 3. Optical probes for UNP's using light resonant with the main transition of Sr^+. (*a*) Absorption imaging: the laser beam is absorbed by the UNP, creating a shadow image that is recorded with a CCD intensified camera. An absorption spectra can be constructed from a series of images, each taken at different laser beam frequencies. From these spectra, plasma parameters such as number of ions and velocity are extracted. (*b*) Fluorescence imaging: the laser beam propagates perpendicularly to the camera and imaging axis. Spectra are constructed in the same fashion as in absorption. With the fluorescence geometry the effects of expansion energy and thermal energy can be decoupled.

- sheet fluorescence imaging is used to study the expansion of the strontium plasma

J.Castro, H.Gao and T.C.Killian, PPCF **50** (2008) 124011

Expansion of an Ultracold Plasma

PRL 99, 155001 (2007) PHYSICAL REVIEW LETTERS week ending 12 OCTOBER 2007

Experimental Realization of an Exact Solution to the Vlasov Equations for an Expanding Plasma

S. Laha,[1] P. Gupta,[1] C. E. Simien,[1] H. Gao,[1] J. Castro,[1] T. Pohl,[2] and T. C. Killian[1]
[1]*Department of Physics and Astronomy, Rice University, Houston, Texas 77005, USA*
[2]*ITAMP, Harvard-Smithsonian Center for Astrophysics, 60 Garden Street, Cambridge, Massachusetts 02138, USA*
(Received 14 May 2007; published 8 October 2007)

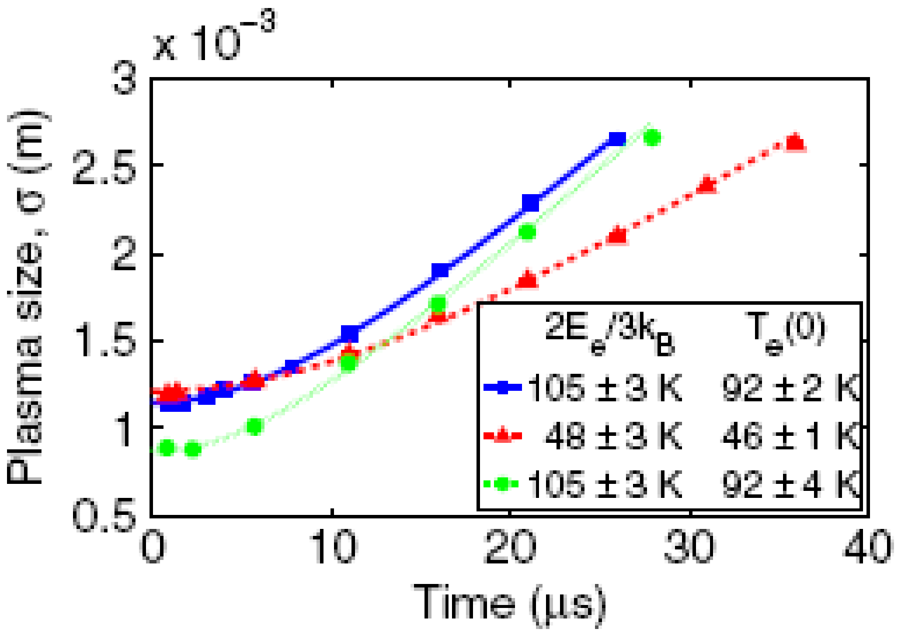

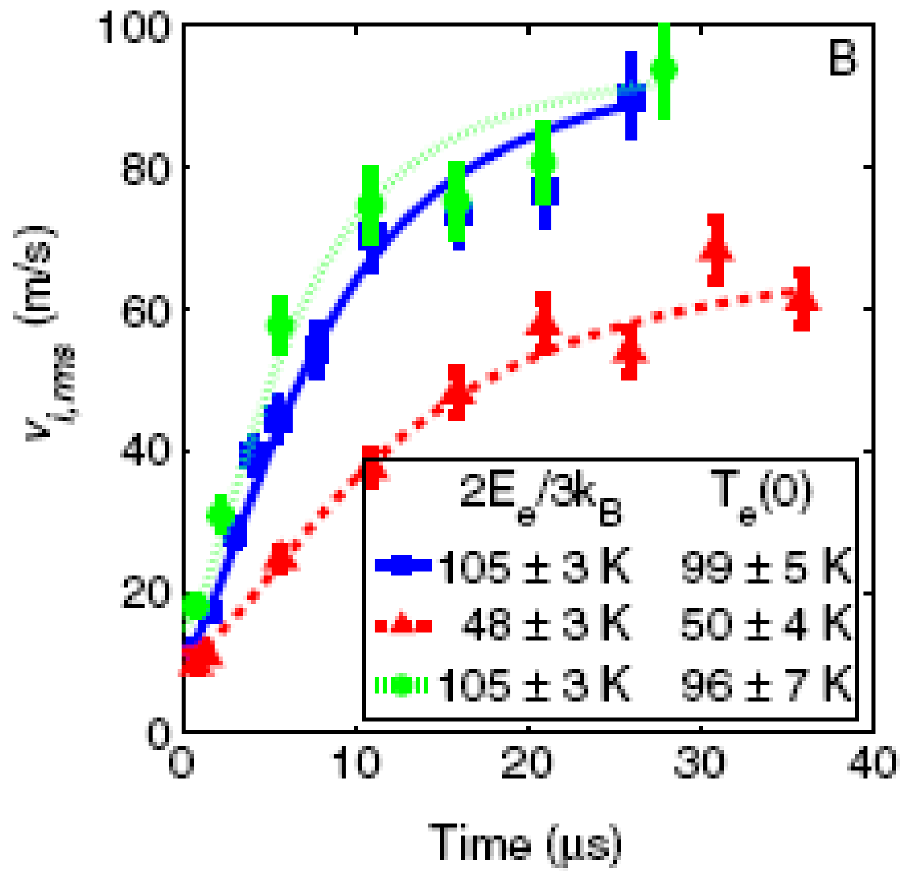

The self-similar solution for a neutral plasma fits well the data for the radius and velocity

Strong coupling effects: kinetic energy oscillations

Ions evolve from an uncorrelated to a correlated distribution converting energy from potential to kinetic (“overshoot” leads to oscillations)

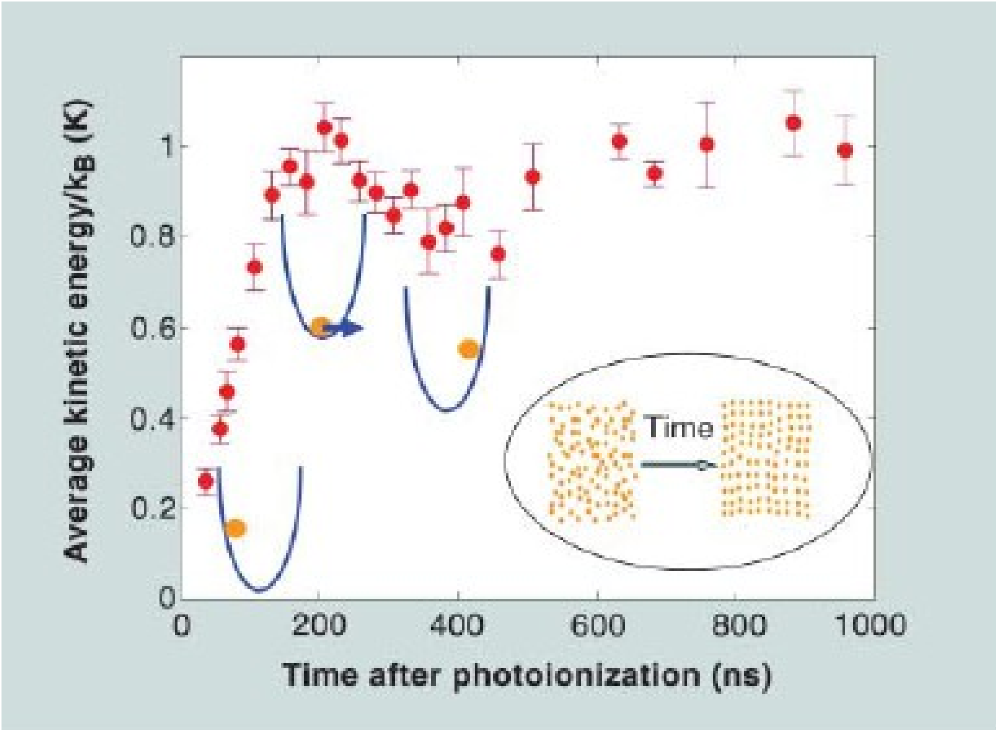

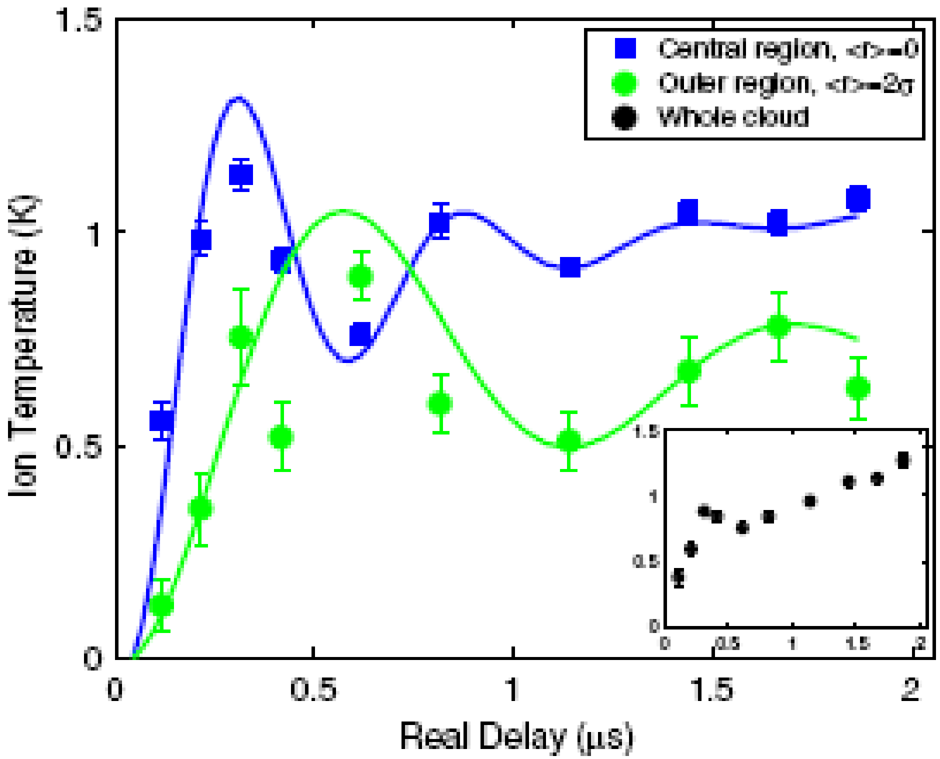

absorption imaging data
(spatially integrated)

fluorescence imaging data
(spatially resolved)

C.E.Simien et al., PRL **87** (2001) 115003
T.C.Killian, Science **316** (2007) 705

J.Castro, H.Gao and T.C.Killian,
PPCF **50** (2008) 124011

Simulations predict plasma crystallization

VOLUME 92, NUMBER 15 PHYSICAL REVIEW LETTERS week ending 16 APRIL 2004

Coulomb Crystallization in Expanding Laser-Cooled Neutral Plasmas

T. Pohl, T. Pattard, and J. M. Rost

Max Planck Institute for the Physics of Complex Systems, Nöthnitzer Strasse 38, D-01187 Dresden, Germany

(Received 26 November 2003; published 16 April 2004)

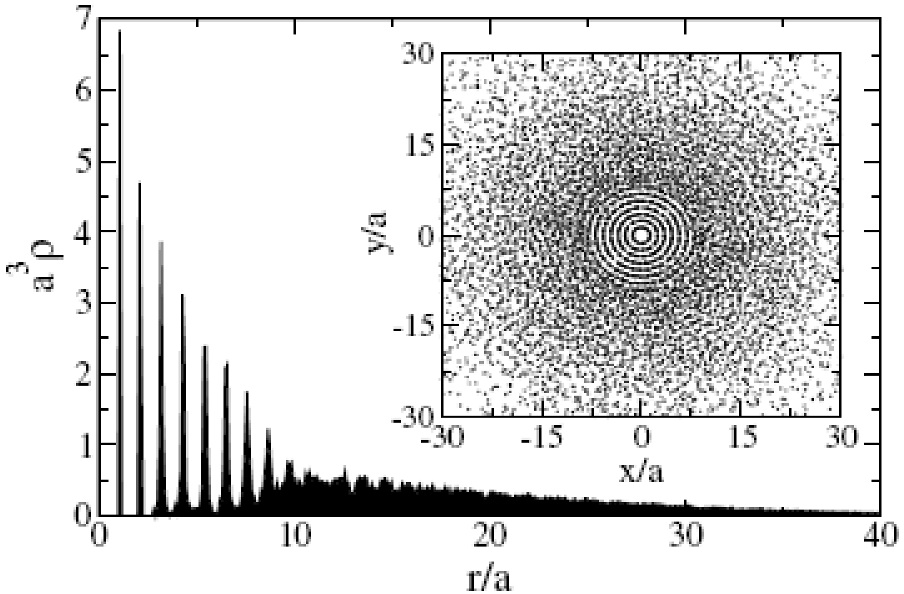

FIG. 3. Radial density after a time of $t = 24\ \mu$s ($\omega_{p0}t = 110$). The inset shows a two-dimensional cut through the plasma cloud, clearly revealing the formation of concentric shells. (For better contrast, cuts with $x = 0$, $y = 0$, and $z = 0$, respectively, have been overlayed.)

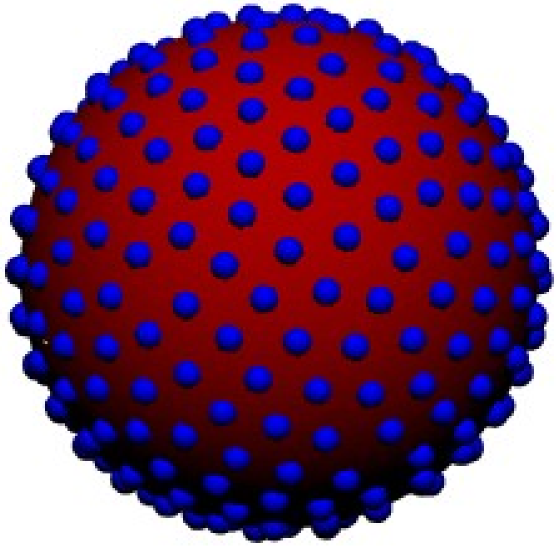

FIG. 4 (color online). The fifth shell of Fig. 3, demonstrating significant intrashell ordering.

not observed in experiments yet...

(see also: T.C.Killian, “Plasmas put in order”, Nature **429** (2004) 815

Future directions and challenges

- Achieving stronger coupling for electrons to drive crystallization
    - laser cooling of the plasma?
    - “enforced” correlations?

- Characterizing collective modes and instabilities (also to provide diagnostics)

- Studying ultracold plasma behavior in strong external magnetic fields

- ...

T.C.Killian, T.Pattard, T.Pohl, J.M.Rost, Phys.Rep. **449** (2007) 77

Conclusions

- Besides the potential applications, “hot” plasmas interacting with superintense laser pulses are of basic interest as a nonlinear, relativistic, “macroscopic”, self-organizing many particle system

- Proton probing techniques with picosecond resolution allowed the detection or detailed studies of many relevant fast phenomena for the first time, stimulating theoretical and computational work

- The limitation is that plasma conditions are not controlled neither characterized with high precision

- Ultracold plasmas are interesting both as a well-controlled, easy-to-diagnose plasma environment for basic physics studies as well as a promising way to create very strongly coupled plasmas in the laboratory

This talk may be downloaded from

www.df.unipi.it/~macchi/talks.html

Electron probing of "colder" plasmas

Picosecond electron deflectometry of optical-field ionized plasmas

MARTIN CENTURION[1*†], PETER RECKENTHAELER[1,2†], SERGEI A. TRUSHIN[1], FERENC KRAUSZ[1,2] AND ERNST E. FILL[1]

[1]Max-Planck-Institut für Quantenoptik, Hans-Kopfermann-Strasse 1, D-85748 Garching, Germany
[2]Ludwig-Maximilians-Universität München, Am Coulombwall 1, D-85748 Garching, Germany

Nature Photonics
2 (2008) 315

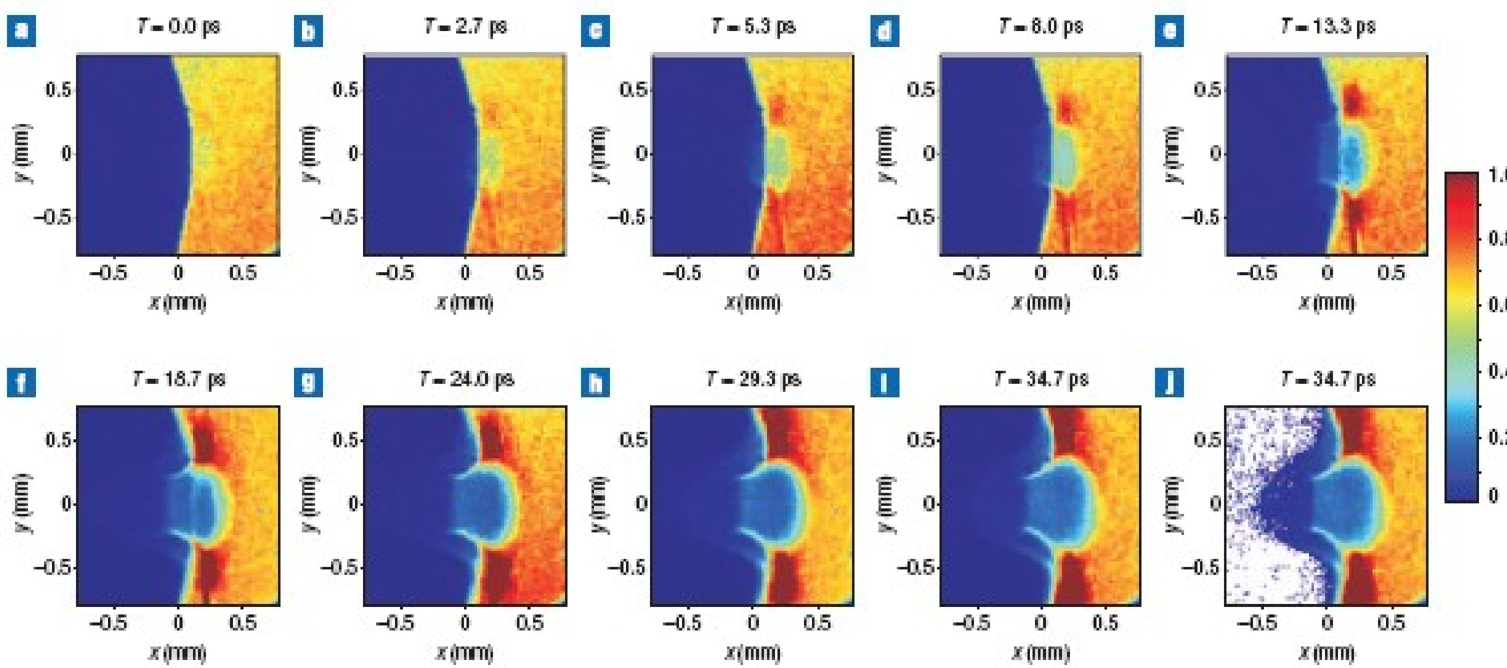

20 keV electrons suitable for measurements of $\boldsymbol{E} \sim 10^7$-10^8 V/cm and $\boldsymbol{B} \sim 10^4$ Gauss

Properties of the proton source

Imaging properties of the emitted protons are those of a **point-like virtual source**

Proton beam is **quasi-laminar** (**ultra-low emittance**)

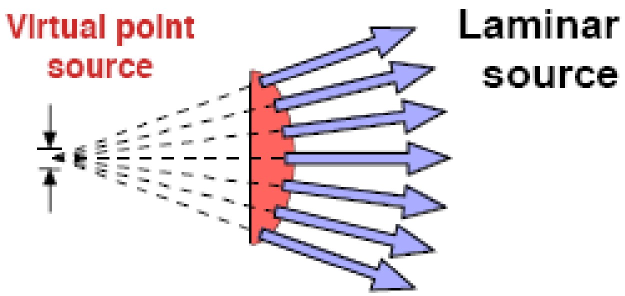

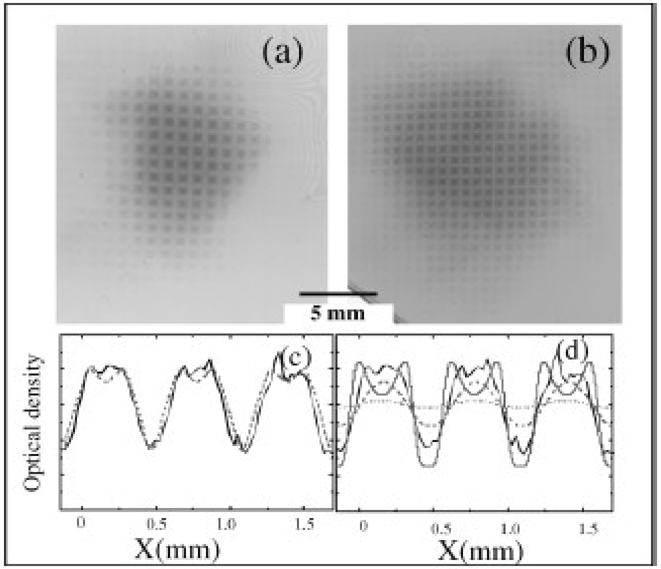

Shadow of micrometric grid mesh with 15 MeV protons provides magnification test and estimate of source dimensions $a < 10\ \mu m$
[Borghesi et al, PRL **92** (2004) 055003]

$a = 1.4\ \mu m$ reported at lower energy
[Cobble et al, J.Appl.Phys. **92** (2002) 1775]

Imaging of thin objects possible due to multiple small-angle scattering of protons
[West & Sherwood, Nature **239** (1972) 157]

Transverse emittance measurement for >10 MeV protons
[Cowan et al, PRL **92** (2004) 204801]

$\varepsilon < 4 \times 10^{-3}$ mm mrad

Study of "coherent", long-lived field structures

Theory and numerical simulations show that a variety of slowly varying structures (**solitons**, **vortices**, **cavitons** ...) is generated during laser-plasma interactions.

Bubble-like structures interpreted as remnants of **relativistic solitons** ("post-solitons")

[Borghesi et al., Phys. Rev. Lett. **88** (2002) 135002]

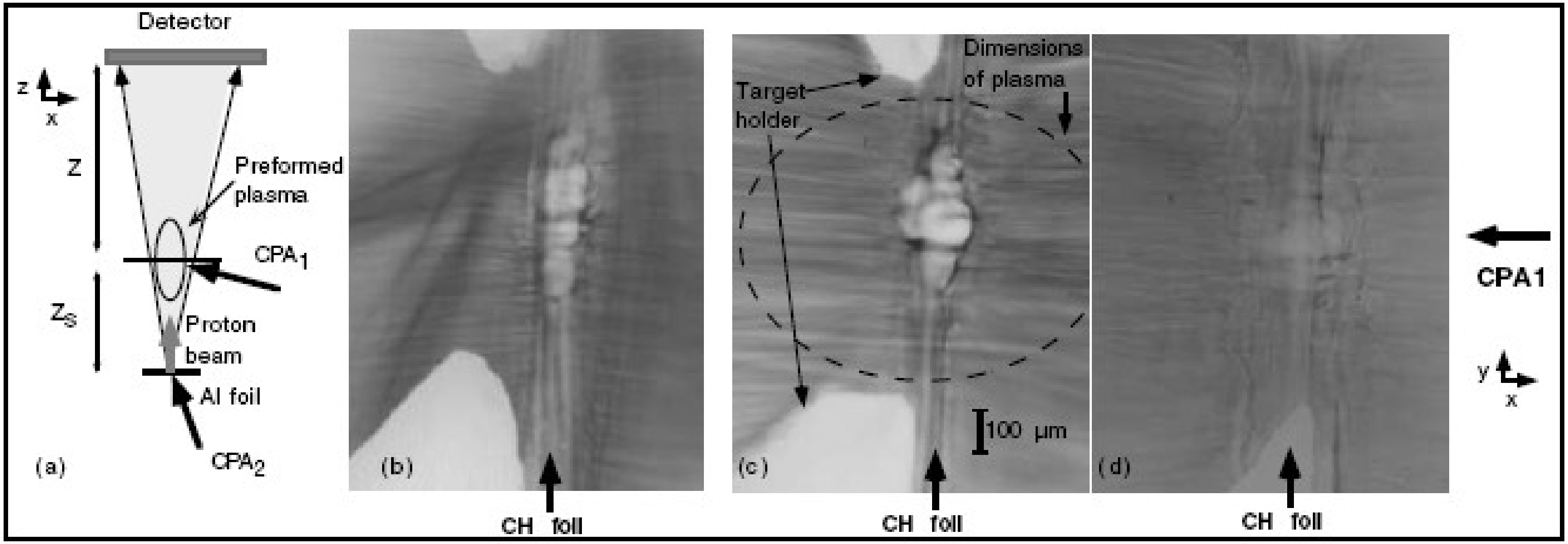

FIG. 1. (a) Experimental arrangement. (b), (c), (d) Proton images of the preformed plasma taken with 6–7 MeV protons, respectively: (b) 25 ps; (c) 45 ps; (d) 95 ps after the CPA$_1$ interaction. The scale refers to dimensions in the object plane. The dashed line indicates the dimensions of the preformed plasma defined by $n \approx 0.01 n_{cr}$ (at $\lambda = 1\ \mu$m).

Study of “coherent”, long-lived field structures

Theory and numerical simulations show that a variety of slowly varying structures (**solitons**, **vortices**, **cavitons** ...) is generated during laser-plasma interactions.

Ion modulations resulting from onset and evolution of **Buneman instability** in the late evolution of a plasma wake

[Borghesi et al., Phys. Rev. Lett. **94** (2005) 195003]

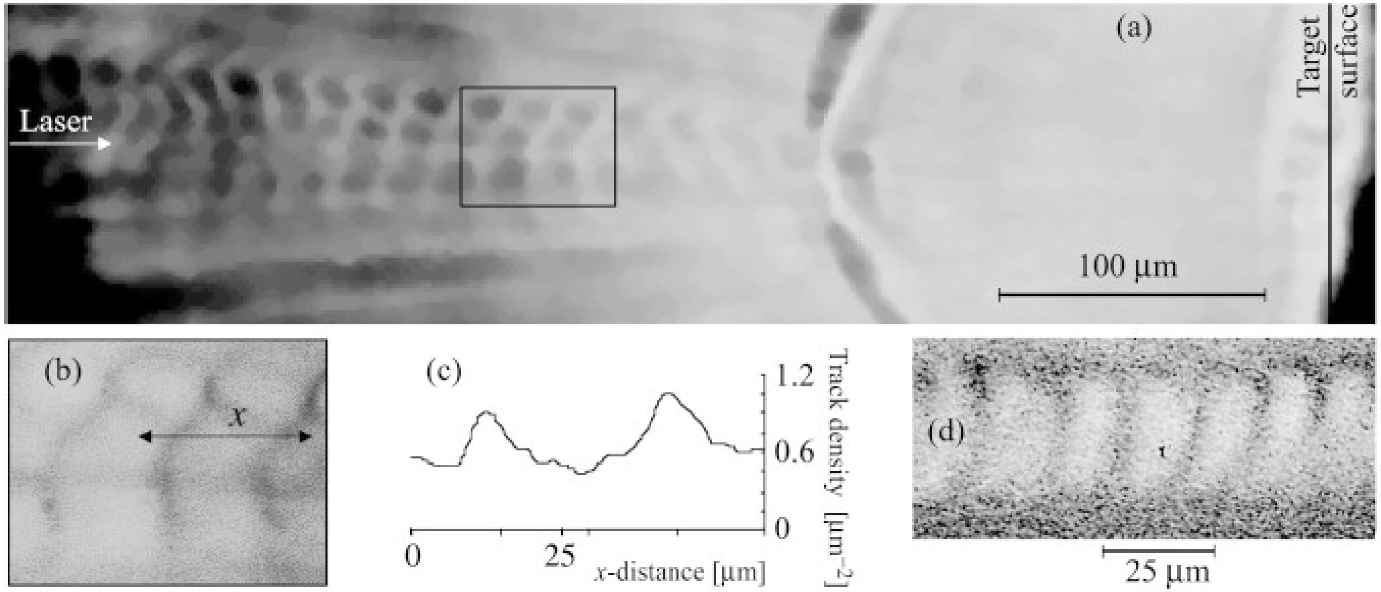

FIG. 1. (a) Proton projection image of the region in front of the laser-irradiated target, taken 20 ps after the interaction. The picture is a reflection scan of the exposed CR 39; (b) Detail of the image in frame (a), (c) Profile of the proton track density along the direction indicated by the arrow in (a); (d) Detail of the pattern observed at the back of a 0.9 μm Mylar target 20 ps after the interaction. The detail shown was located at a distance of about 200 μm from the original target plane.

Study of "coherent", long-lived field structures

Theory and numerical simulations show that a variety of slowly varying structures (**solitons**, **vortices**, **cavitons** ...) is generated during laser-plasma interactions.

Regular, quasi-periodic structures observed inside or near the charge-displacement channel at late times

[T.V.Lyseikina, F.Ceccherini, F. Cornolti, E.Yu.Echkina, A.Macchi, F.Pegoraro, M.Borghesi, S.Kar, L.Romagnani, S.V.Bulanov, O.Willi, M.Galimberti, arXiv:physics/0701139]